CNWRA *A center of excellence in earth sciences and engineering™*

Geosciences and Engineering Division
6220 Culebra Road • San Antonio, Texas, U.S.A. 78238-5166
(210) 522-5160 • Fax (210) 522-5155

July 29, 2009
Contract No. NRC–02–07–006
Account No. 20.14003.01.007
NMSS06n: PROJ0734; PROJ0735

ATTN: Document Control Desk
U.S. Nuclear Regulatory Commission
Mr. Michael L. Fuller
Division of Waste Management and Environmental Protection
Two White Flint North; Mail Stop T7–J8
11555 Rockville Pike
Washington, DC 20852

Subject: Revised Mesoscale Grout Monolith Experiments: Results and Recommendations (Deliverable 14003.01.007.305)

Dear Mr. Fuller:

This letter transmits the revised report Mesoscale Grout Monolith Experiments: Results and Recommendations. This work was undertaken to better inform the U.S. Nuclear Regulatory Commission's (NRC's) understanding of the behavior and sealing properties of grout formulations the U.S. Department of Energy (DOE) is considering for closure of radioactive waste tanks at sites specified in the Ronald W. Reagan National Defense Authorization Act of Fiscal Year 2005.

This report describes the methods used to construct grout specimens on the scale of 55-gallon drums and a 3-m [10-ft] radius, 30° arc specimen using a variety of grout formulations DOE is considering. The report describes our observations with respect to the physical properties and behavior of the grout formulations, such as flow characteristics and water/aggregate segregation, the thermal behavior of the grout during curing, visual observations of cracks and voids present in the solidified specimens, and the results of gas injection tests to evaluate the permeability of the specimens.

The draft report has been revised in response to NRC comments received on June 26, 2009, and in light of information gathered at the Cementitious Barriers Partnership Workshop on Development of Test Beds on July 15–16, 2009, and "draft" has been removed from the title of the report. We look forward to continuing to support NRC work in this important area with additional experiments and related analysis and interpretations.

Please do not hesitate to contact me (301.881.0290) or Dr. Gary Walter (210.522.3805) with any questions about the subject report.

Sincerely,

John Stamatakos, Ph.D.
Director,
Rockville Office and
Environmental Program

EP/JS/ls-attachment; enclosure

cc:				email:	
	D. DeMarco	A. Kock	G. Walter		
	S. Kim	C. Barr	C. Dinwiddie	W. Patrick	GED Managers
	V. Whipple	C. McKenney	J. Stamatakos	B. Sagar	L. Naukam
	P. Bubar	C. Grossman		GED Directors	Record Copy B—IQS

Washington Office
1801 Rockville Pike, Suite 105 • Rockville, Maryland 20852-1633

Resolution of Comments on Draft Mesoscale Grout Monolith Experiments: Results and Recommendations (Deliverable 14003.01.007.300) (Responses in Italics)

General

1. The report is very well written and the evaluations well thought out. Experimenters showed initiative in designing the experiments and analyzing the results.

***Response**: The experimenters appreciate the U.S. Nuclear Regulatory Commission's (NRC) kind comment.*

2. We strongly support further research to address the last two recommendations listed in Section 4.0.

***Response**: Comment will be incorporated into future plans.*

3. On pages 6, 13, 15, and 39 of the report, the text describes the Center for Nuclear Regulatory Analyses' (CNWRA) need to withhold a portion of the prescribed water to achieve desired flowability. However, in future experiments the CNWRA should consider (i) further evaluation of the disparity in the actual water content used for the U.S. Department of Energy (DOE) grouts versus those used in CNWRA cement formulations and/or (ii) use grout formulations consistent with DOE specifications.

***Response**: It was our understanding that DOE put preference on meeting the desired ASTM flow characteristic expectations over keeping to the nominal water specified by a given grout formulation; thus, we did the same. The water content of the grout formulations was adjusted from the nominal amounts reported in the DOE grout formulation sources in an attempt to meet the flow specifications without water/solid segregation. This adjustment was made recognizing that the materials used in the CNWRA experiments were not exactly the same as those various DOE experimenters used (e.g., different source of Portland cement, different source of fly ash, different batch sizes, and, possibly, different humidity conditions in the experimental facility). One outcome of the Cementitious Barriers Partnership Workshop on Development of Test Beds was the new understanding that DOE puts equal weight on meeting both the grout formulation and the grout flowability specifications. More experimental work may be needed before we can satisfactorily attain the desired grout flowability in the absence of solid–liquid segregation while using the full volume of water DOE specified. Annulus apertures measured via our experiments may underestimate the size of apertures that would develop had DOE's full volume of nominal water been used in all grout formulations. NRC's comment is well taken, and future experiments will consider the effect of using exact DOE formulations on the properties of the grout specimens and bonds between grout and walls or internal fixtures.*

Specific

1. Page 1, 2nd paragraph, last sentence. The text states, "To this end, the ... CNWRA... has been tasked to provide mechanistic information on the physical and chemical degradation of cementitious waste forms that are used for the isolation and containment of radioactive wastes, and to evaluate the potential for radionuclide bypass of the engineered barriers...." Limitations to this tasking include difficulty in simulating long-term degradation processes, as well as difficulty in simulating the actual scale of the real systems being studied as discussed on page 2. Suggest including a similar discussion

regarding the limitations of the experiments to study the long-term degradation processes within the constraints of the short-term experiments.

***Response**: Suggested discussion has been added to Section 1, and a recommendation has been added to repeat the gas injection tests after 6 to 9 months to evaluate the effects, if any, of long-term curing of the specimens.*

2. Page 9, 1st (incomplete) paragraph. There is discussion on page 9 regarding ambiguity in the heel grout formulation used for INL tanks. Two references are cited that contain different specifications for water and high-range water reducer (i.e., ADVA 380) quantities per 3 ft^3 batches. Upon request, in early 2009 NRC staff provided CNWRA with a batch ticket for an actual engineered grout pour (or heel grout) used in grouting the large tanks at the Idaho National Laboratory (INL). It is not clear how the actual formulation used at INL compares to the final grout formulation used for the experiments. The final grout formulation used to grout INL tanks should be consistent with INL specifications as verified in the field during an onsite observation; and the Waste Management reference (Langton and Cook, 2007) should not be considered a reliable source of information for future experiments.

***Response**: We compared the batch ticket for Heel Displacement Grout Mix #6 (Valley Ready Mix April 16, 2007) with the formulation Langton and Cook (2008) reported and found the only differences were (i) 230 lb/yd^3 of Portland cement was called for in the batch ticket versus 227 lb/yd^3 reported by Langton and Cook (2008) and (ii) Valley Ready Mix used 38 oz/yd^3 of Glenium 3030 as the high range water reducer, whereas we used 80 oz/yd^3 of ADVA 380. The grout specification allows the high range water reducer to be adjusted to meet the required slump. The text on page 9 has been modified to clarify some of these issues. We can investigate the effect of these differences in future experiments.*

3. Page 39, 1st complete paragraph, 2nd sentence: The text states "In addition, the water required to achieve a specific flowability varied between batches and a slight excess of water led to segregation of water and grout solids." Suggest adding additional text explaining the risk significance of water and grout solid segregation.

***Response**: Text has been added to indicate that segregation and water bleeding can produce layers with increased porosity and permeability that can be pathways for fluids to enter the grout and transport of radionuclides.*

4. Pages 38–41, Section 4 "Conclusions and Recommendations." Suggest including a recommendation to test samples under a higher temperature gradient to investigate whether there is a threshold for induction of thermal cracking; and to test whether there are scale effects associated with this phenomena. Also consider thermal-mechanical modeling to aid in the experimental design (e.g., investigate the conditions where thermal cracking may occur).

***Response**: The recommendation related to thermal gradients has been modified to propose using external heat sources to create larger thermal gradients and comparison of thermo-mechanical modeling simulations with the experimental results.*

Recommendations

1. Page 26, 2nd paragraph. CNWRA discusses the addition of poorly sorted red sand to evaluate the ability of the grout to move particulate matter. While the issue of residual sludge displacement by grout is important, it is not clear if sand would closely approximate the flow characteristics of sludge. Consider use of more representative sludge analogs if any future experiments to further study the characteristics of waste/grout mixing are conducted.

***Response**: If any future experiments to study the characteristics of waste/grout mixing are conducted, we will further investigate the characteristics of tank sludge to find an appropriate analog material.*

2. The kinetics of fly ash and slag hydration are typically slower than that of Portland cement. Accordingly, the experiments resulted in suppressed grout temperatures for the samples with fly ash and slag. As temperatures approach 60 °C, however, slag and fly ash hydration kinetics (which are more temperature dependent than Portland cement) increase to the point of approximating that of Portland cement. Although the volume of cement inside the of 55-gal drums used in the experiments may not provide ample feedback for accelerated hydration kinetics for pozzolanic materials, a DOE tank may. If future small-scale experiments are conducted, suggest considering methods to maintain the drums (or future specimens) at ~40–60 °C while they cure to evaluate the potential for more rapid hydration of slag and fly ash and therefore a greater ultimate reaction temperature.

***Response**: When planning for future small-scale experiments, we will consider the feasibility of using external heat sources to more fully investigate the effect of more rapid thermal hydration and higher reaction temperatures on cracking. A recommendation to this effect has been added to the report.*

Editorial

1. Page 29, 1st paragraph. Suggest providing a better description of the rheological behavior of freshly mixed grout with water-to-cement ratios of less than 2 (i.e., the reader may not be familiar with this property for fresh pahoehoe lava below the liquidus temperature).

***Response**: An analogy between the flow behavior of grout and lava was developed for the benefit of earth scientists and members of the public who may be more familiar with the characteristics of lava than they are with the characteristics of fresh grout. The analogy was not a necessary component of the report, but was simply intended to provide a useful point of comparison for an expected subset of the report's readership. Those readers who are familiar with the theology of grout need no such comparison and can quickly skim over this sentence.*

Other Changes

1. *Three typographical errors at the bottom of page 1 have been corrected.*

2. *The wording of the last sentence on page 1 referring to the "grout compositions conformed to grout formulations ..." was changed to "grout compositions were consistent with ..."*

3. *The lower water-to-cement ratio we used when mixing grouts was addressed on page 6 in a clarification of existing text:*

   "The masses and volumes of the grout ingredients were determined by proportionately adjusting the quantities DOE reported for specific grout formulations (Table 3-2) to meet a final volume of approximately 0.085 m^3 [3 ft^3]. Each grout batch varied slightly in material quantities from the nominal formulation recipe and varied more significantly in the water quantity; specifically, to meet the flowability specifications, we had a lower water-to-cement ratio in every case."

4. *We have clarified the discussion on page 7 of the adjustment of the INL CLSM Grout formulation to meet the volume requirements for filling the drum specimens.*

5. *Text at the bottom of page 26 and the top of page 28 was removed because it should not have been included in the original draft report, per email from C. Dinwiddie to L. Selvey dated May 18, 2009. Thus, the following text was deleted from the final report:*

   "Focused examination of crack formation in this grout lift revealed that INL CLSM Grout, which underwent solid–liquid segregation upon emplacement, experienced significant swelling overnight. Photographs of the first lift immediately after emplacement indicate that the grout level in the drum did not rise high enough to contact the gas injection pipe; however, by the next morning, the grout had swelled sufficiently to make contact with the bottom of the gas injection. As explained by Neville (2006), grout cured in water increases in volume and mass due to absorption of water by cement gel."

6. *Text at the bottom of page 31 was clarified:*

   "Grouted pipes were later tested in the same way to determine whether internal annuli had developed between the pipe grout and pipe wall."

7. *Text summarizing calculated apparent apertures (in the two full paragraphs at the bottom of page 33) was clarified:*

   "With one exception, the calculated annulus apertures for the drum grout specimens are relatively consistent, ranging from 1 to 18 μm [39 to 710 μin]. INL CLSM Grout specimens developed the smallest apparent apertures, and the largest apparent aperture developed in a drum of SRS Strong Grout (Table 3-6). The 78-μm [3070-μin] "aperture" computed for drum grout specimen T6 (Table 3-6) is clearly influenced by both annular and diffuse flow through the grout based on visual and audible observation of gas emerging from an annulus between the grout and drum wall (unlike the other specimens from which gas emerged from an annulus between the grout and the gas injection pipe). The apertures computed for drum grout specimens T1, T2, and T8 may also be influenced by diffuse flow based on visual observations that gas, which emerged around the pipe, appeared to be less than the total measured gas flow rate. In the case of drum grout specimen T7, no gas flow was observed around the pipe."

   The apertures computed from the sector specimen tests were consistently at the high end of the drum specimen scale, ranging from approximately 14 to 20 μm [550 to 790 μin]. The larger calculated aperture values for the sector grout specimen are consistent with visual observation of macroscopic annuli around the sector specimen

gas injection pipes. The larger annuli for the sector specimen may be due to the greater potential for hydration shrinkage and thermal contraction in the sector grout specimen compared to that of the drum grout specimens due to the sector specimen's greater volume. However, note that one drum specimen of SRS Strong Grout did have an apparent aperture of this magnitude, so one cannot rule out the possibility that the grout formulation itself may have had a role in the size of the annulus that developed."

8. *Table 3-7 was made consistent with Table 3-6 by removing the redundant word "Grout" from many entries where it was not needed.*

9. *The permeability for our monofill INL Heel Grout specimen was reestimated by simulating gas flow assuming an annular space at the drum wall. The revised estimates are slightly lower, and Table 3-8 was updated with the revised values.*

10. *A recommendation was added to page 41 to repeat the gas injection tests on the grout specimens after 6 to 9 months of curing to detect any change in properties due to curing.*

MESOSCALE GROUT MONOLITH EXPERIMENTS: RESULTS AND RECOMMENDATIONS

Prepared for

U.S. Nuclear Regulatory Commission
Contract NRC–02–07–006

Prepared by

Gary R. Walter
Cynthia L. Dinwiddie
Emily J. Beverly
Donald Bannon
Deborah Waiting
Greg Bird

Center for Nuclear Waste Regulatory Analyses
San Antonio, Texas

July 2009

PREVIOUS REPORTS IN SERIES

Number	Name	Date Issued
14003.01.007.222	Conceptual Design for Small-Scale Grout Monolith Tests	April 2008

CONTENTS

Section Page

PREVIOUS REPORTS IN SERIES ii
FIGURES iv
TABLES v
ACKNOWLDGMENTS vi

1 BACKGROUND AND SCOPE OF REPORT 1

2 REVIEW OF DESIGN CONSIDERATIONS FOR MESOSCALE GROUT MONOLITH EXPERIMENTS 2

3 TEST PLAN IMPLEMENTATION 3
3.1 Preparation of Mesoscale Grout Monolith Test Specimens 4
3.1.1 Thermal Expansion and Contraction Specimens 4
3.1.2 Thermal Hydration and Drying Shrinkage Specimen 11
3.1.3 Pipe Grout Specimens 15
3.2 Thermal Evolution of Grout Monolith Specimens 15
3.2.1 Thermal Expansion and Contraction Specimens 15
3.2.2 Thermal Hydration and Drying Shrinkage Specimen 19
3.2.3 Pipe Grout Specimens 19
3.3 Analyses of Potentially Conductive Pathways in Grouted Test Specimens 24
3.3.1 Visual Inspection and Borescopic Observations 26
3.3.2 Gas Injection Testing 31
3.3.3 Annular Aperture Analysis 32
3.3.4 Effective Gas Permeability Analysis and Estimates 34

4 CONCLUSIONS AND RECOMMENDATIONS 39

5 REFERENCES 41

6 APPENDIX A A–1

FIGURES

Figure Page

2-1 Illustration of Experimental Test Specimen Plan-View Scales Relative to Nominal Plan-View Scale of an NDAA Waste Tank 2

3-1 Plan View of CNWRA Mesoscale Grout Monolith Laboratory and Office Space With Photographic Inset of Drum Grout Specimens 3
3-2 Relative Placement of Thermocouples in a Typical Drum Grout Specimen 7
3-3 Pictorial Overview of Preparation of Drum Grout Specimen T9 10
3-4 Plan View of Grout Sector Specimen Showing Approximate Locations of Gas Injection Pipes (Open Circles) and Thermocouples (Colored Squares) 12
3-5 Pictorial Overview of Preparation of Sector Grout Specimen 14
3-6 Thermal Evolution of Grout Curing in SRS Strong and Reducing Grout Drum Specimens 16
3-7 Thermal Evolution of Grout Curing in SRS Alternative Grout Drum Specimens 17
3-8 Thermal Evolution of Grout Curing in INL Grout Drum Specimens 18
3-9 Thermocouple Response Keyed to Thermocouple Location in SRS Strong and Reducing Grout Drum Specimens 20
3-10 Thermocouple Response Keyed to Thermocouple Location in SRS Alternative Grout Drum Specimens 21
3-11 Thermocouple Response Keyed to Thermocouple Location in INL Grout Drum Specimens 22
3-12 Select Temperature Gradients. 23
3-13 Thermal Evolution of Sector Specimen 24
3-14 Thermal Evolution of Pipe Grout 25
3-15 Grout Surface Features 27
3-16 Downhole Borescope Photographs of Grout Details 30
3-17 Illustration of the Finite Volume Grid Used for Drum Gas Flow Simulations 36
3-18 Correlation Between Gas Flow and Grout Effective Gas Permeability Developed for Drum Grout Specimens 37

TABLES

Table Page

3-1 Matrix of 55-gal Drum Test Specimens for Testing Thermal Expansion/Contraction Effects on Pipe–Grout Bonds 4
3-2 U.S. Department of Energy Grout Formulations for 3-ft^3 Batches 5
3-3 Summary Statistics of Grout Batch Ingredient Quantities and Resulting Bulk Densities for Drum-Scale Specimens 8
3-4 Summary Statistics of Grout Batch Ingredient Quantities and Resulting Bulk Densities for ¼-Scale Sector Specimen 13
3-5 Drum Grout Lift Surface Texture Characteristics 28
3-6 Calculated Average Annular Apertures Between Injection Pipe and Drum or Sector Grout 33
3-7 Calculated Average Annular Apertures Between Idaho National Laboratory (INL) Pipe Grout and Injection Pipe 35
3-8 Calculated Effective Gas Permeabilities for Selected Drum Grout Specimens 38

ACKNOWLEDGMENTS

This report was prepared to document work performed by the Center for Nuclear Waste Regulatory Analyses (CNWRA®) for the U.S. Nuclear Regulatory Commission (NRC) under Contract No. NRC–02–07–006. The activities reported here were performed on behalf of the NRC Office of Federal and State Materials and Environmental Management Programs, Division of Waste Management and Environmental Protection. This report is an independent product of CNWRA and does not necessarily reflect the view or regulatory position of NRC.

The authors wish to thank R. Brient for his quality assurance oversight and audit, L. Mulverhill for her editorial review, R. Pabalan for his technical review, B. Sagar for his programmatic review, and L. Selvey for her secretarial support. The authors also thank Boral Material Technologies, Inc. and CP Kelco for providing fly ash and Kelco-crete® for these experiments at no cost.

QUALITY OF DATA, ANALYSES, AND CODE DEVELOPMENT DATA

DATA: All CNWRA-generated data contained in this report meet quality assurance requirements described in the Geosciences and Engineering Division Quality Assurance Manual. Sources of other data should be consulted for determining the level of quality of those data. The work presented in this report is documented in Scientific Notebooks 960E (Dinwiddie, et al., 2009), 963 (Walter, et al., 2009a), 971 (Walter, et al., 2009b), and 974 (Walter, 2009).

ANALYSES AND CODES: The BioGas Emissions Model (BIGEM) code (Walter, 2005) was used to generate results for this report and is controlled in accordance with the CNWRA Technical Operating Procedure (TOP)–018, Development and Control of Scientific and Engineering Software.

References:

Dinwiddie, C.L., G.R. Walter, E.J. Beverly, and D.R. Bannon. “Grout Monolith Electronic Data Files.” Electronic Scientific Notebook 960E. San Antonio, Texas: CNWRA. 2009.

Walter, G. “Grout Studies.” Electronic Scientific Notebook 974. San Antonio, Texas: CNWRA. 2009.

Walter, G.R. “BioGas Emissions Model (BIGEM) Version 1.00 Software Validation Test Plan and Report.” San Antonio, Texas: CNWRA. 2005.

Walter, G., D. Bannon, C. Dinwiddie, E. Beverly, and G. Bird. “Small-Scale Grout Experiments.” Scientific Notebook 963. San Antonio, Texas: CNWRA. 2009a.

Walter, G., E. Beverly, D. Bannon, and C. Dinwiddie. “NDAA Grout Experiments.” Scientific Notebook 971. San Antonio, Texas: CNWRA. 2009b.

1 BACKGROUND AND SCOPE OF REPORT

Under Section 3116 of the Ronald W. Reagan National Defense Authorization Act of Fiscal Year 2005 (NDAA), the U.S. Nuclear Regulatory Commission (NRC) is responsible for consulting with the U.S. Department of Energy (DOE) on DOE's waste determinations for certain waste tanks and vaults at the Savannah River Site (SRS) and Idaho National Laboratory (INL), and for monitoring disposal actions taken by the DOE pursuant to NDAA, Section 3116, Subsection (a)(3), Subparagraphs (A) and (B) to assess compliance with the performance objectives of 10 CFR Part 61, Subpart C. The NDAA provides criteria to determine whether certain waste resulting from the reprocessing of spent nuclear fuel is not high-level waste and specifies that DOE must meet the performance objectives in 10 CFR Part 61, Subpart C.

Under the provisions of this Act, DOE has been stabilizing and will continue to stabilize waste tanks and vaults with cementitious materials such as grout. Cementitious materials may be formulated to produce waste forms that enhance waste isolation by limiting radionuclide release and migration. DOE may rely on (i.e., take credit for) natural and engineered system properties that may provide attenuation and retardation of radionuclide migration as part of their waste disposal system performance assessments. NRC staff need information from independent analyses that support their consultation responsibilities for non-high-level, waste-incidental-to-reprocessing determinations and their monitoring responsibilities for subsequent actions taken under the NDAA. To this end, the Center for Nuclear Waste Regulatory Analyses (CNWRA®) has been tasked to provide mechanistic information on the physical and chemical degradation of cementitious waste forms that are used for the isolation and containment of radioactive wastes, and to evaluate the potential for radionuclide bypass of the engineered barriers via preferential or fast pathways.

Previous reviews of DOE waste determinations indicated that potential fast pathways going through and bypassing barriers may dominate waste release from large, grout-filled tanks and vaults. Thus, macrocrack spacing and geometry may play a major role in the release of radionuclides from in-place tank closures. Review of experimental and observational data on mass transport properties of cementitious materials did not reveal any empirical data from which to estimate the likely properties of macrocracks that may develop in large grout monoliths. Most crack characterization measurements to date have been made on small-scale laboratory specimens using construction materials with significantly different formulations than those DOE proposed for radioactive waste disposal at NDAA facilities. Additionally, no data are available to assess the significance of annular spaces that may develop between cementitious grout and internal tank fixtures (e.g., interior tank walls, pipes, and cooling coils). Lack of relevant data represents a key uncertainty when evaluating DOE waste determinations that rely on cementitious grout integrity to meet the performance objectives for low-level waste found in 10 CFR Part 61, Subpart C.

To establish a base-level understanding of the potential for fast flow cracks and annular separations that may form soon after grout is emplaced in a waste tank, CNWRA staff developed 13 mesoscale cementitious grout monolith specimens at Southwest Research Institute® (SwRI®) facilities in San Antonio, Texas, as analogs to grouted tanks at NDAA facilities. CNWRA staff implemented the conceptual design for grout experiments in fiscal year 2009 that they had previously developed in fiscal year 2008 (Walter and Dinwiddie, 2008) to help inform development of a next-generation conceptual design for larger scale grout monolith experiments. To the extent practical, test bed components were constructed with internal fixtures to represent features of a real waste tank system (e.g., pipes and cooling coils), and grout compositions were consistent with grout formulations being considered by DOE. The

mesoscale grout monolith experiments were constructed and instrumented to permit (i) observation and quantification of the effects of macrocracks, annuli between grout and internal fixtures or external walls, and lift separations that may develop due to thermal contraction cracking, shrinkage, and the passage of time between lift emplacements and (ii) the conduct of gas permeability tests. This letter report fulfills the requirement for CNWRA to document the results of these experiments and to provide recommendations for future work, as funding permits, later this fiscal year and in fiscal year 2010.

2 REVIEW OF DESIGN CONSIDERATIONS FOR MESOSCALE GROUT MONOLITH EXPERIMENTS

Physical scaling issues were well considered during development of the test plan for mesoscale grout experiments. The physical dimensions of waste tanks at NDAA facilities and the practical dimensions of mesoscale test specimens are significantly different (Figure 2-1). Upon considering the physical–chemical thermal hydration processes involved in grout curing, rigorous scaling of mesoscale specimens to duplicate temperatures, temperature gradients, thermal stresses, strains, and shrinkage behavior that might occur in actual DOE grout emplacements was determined not to be possible. For this reason, larger scale experiments are recommended as a next step to more accurately predict and quantify the potential for preferential flow path development at the waste tank scale. In addition to limitations related to the spatial dimensions of the experimental specimens, the short duration of the experiments necessarily limited the changes that could be observed to near-term physical–chemical modifications of the grout as it began to cure. These limitations do not diminish the importance of these preliminary mesoscale experiments, however. These experiments provided (i) staff with first-order experience in mixing and emplacing six different DOE tank grout formulations, (ii) insights into the different formulations' emplacement and curing behaviors, and (iii) a baseline of information from which to design larger scale experiments. In addition, these experiments provided baseline information on the effects of thermal expansion and contraction, and hydration and drying shrinkage on bonding between pipes, tank walls, and grout.

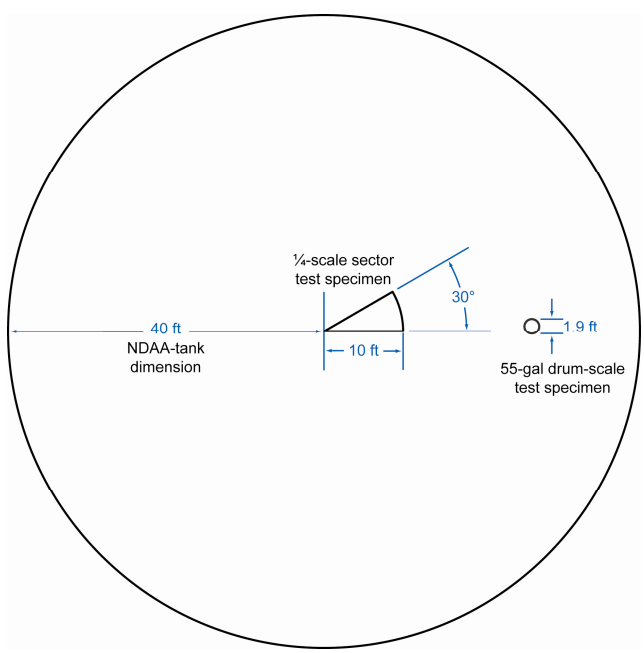

Figure 2-1. Illustration of Experimental Test Specimen Plan-View Scales Relative to Nominal Plan-View Scale of an NDAA Waste Tank. Note: 3.3 ft = 1.0 m.

3 TEST PLAN IMPLEMENTATION

The mesoscale grout monolith experimental laboratory is located just off the main SwRI campus in a high-bay building located at 9800 West Commerce Street, San Antonio, Texas (Figure 3-1).

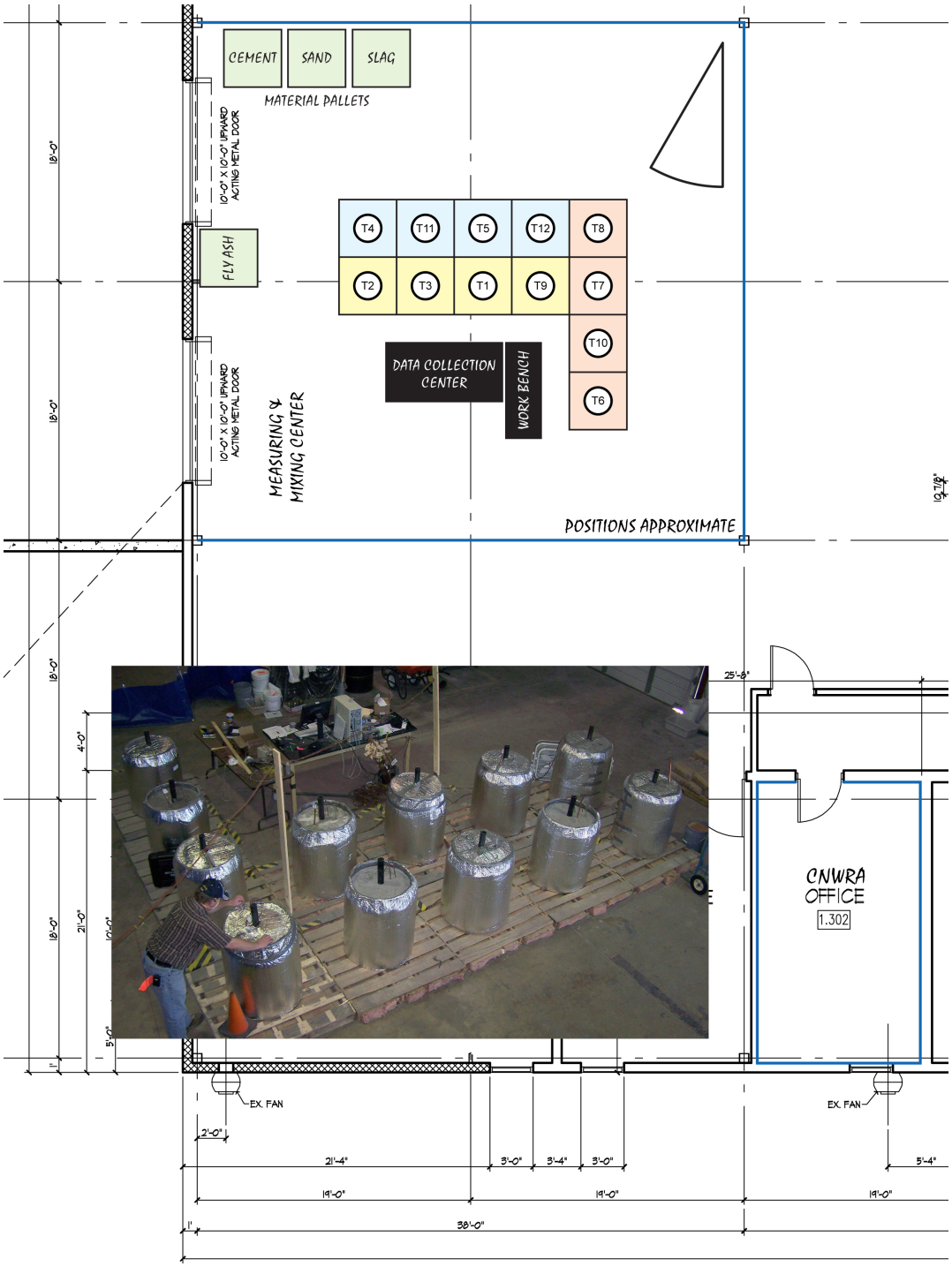

Figure 3-1. Plan View of CNWRA Mesoscale Grout Monolith Laboratory and Office Space With Photographic Inset of Drum Grout Specimens. Note: 3.3 ft = 1 m.

3.1 Preparation of Mesoscale Grout Monolith Test Specimens

3.1.1 Thermal Expansion and Contraction Specimens

Twelve mesoscale cylindrical grout specimens were prepared inside 55-gal drums to investigate effects of thermal expansion and contraction on bonds between pipes, cooling coils, tank walls, and grout (Table 3-1). The specimens were prepared in SKOLNIK open-head carbon steel drums (Skolnik Industries, 2008) with an internal diameter of 56 cm [22.5 in] and internal height of 83.8 cm [33 in]. Black steel schedule 40 pipe {5-cm [2-in] inner diameter} and 1.3 cm [0.5 in] copper tubing were suspended in the drums (Table 3-1) prior to grout pours to simulate pipe fixtures and cooling coils inside NDAA waste tanks. The bottom of the black steel pipe in each specimen was temporarily sealed with a removable plug during grout emplacement and early curing. Borosilicate glass tubing with a flat, closed bottom, flared top, and internal diameter of 25 mm [1 in] (Specialty Glass Inc., Houston, Texas) was also suspended in certain drums to later enable downhole boroscopic observation of features such as cracks, annuli, and lift interfaces (Table 3-1). After initial permeability testing, the central pipes of six specimens were grouted, while others remain open (Table 3-1).

Grout was emplaced in three separate, nominally 25-cm [10-in]-thick lifts into each drum, typically on consecutive days, but occasionally with more elapsed time to simulate the approximate rate at which NDAA waste tanks could be filled. The test specimens are composed of the six DOE grout formulations listed in Tables 3-1 and 3-2.

Because the drum grout specimens were intended to be analogs to grout in the interior of a large grout mass, the circumference and base of the drums were insulated to reduce heat loss and thus to produce internal temperatures similar to those expected inside NDAA waste tanks. Four test specimens were left open to the atmosphere; the other eight were covered with

Table 3-1. Matrix of 55-gal Drum Test Specimens* for Testing Thermal Expansion/Contraction Effects on Pipe–Grout Bonds

Test Specimen	Grout Formulation			Tank Top Insulated?	Copper Tubing?	Glass Borescope Tubing?	Central Pipe Filled?
	Lift 1	Lift 2	Lift 3				
T1	Savannah River Site (SRS) Strong			✓			
T2	SRS Reducing	SRS Strong		✓			✓
T3	SRS Reducing			✓	✓	✓	✓
T4	SRS Alternative 1			✓	✓		✓
T5	SRS Alternative 2			✓		✓	✓
T6	Idaho National Laboratory (INL) Heel			✓			✓
T7	INL Controlled Low Strength Material (CLSM)			✓			
T8	INL Heel	INL CLSM		✓	✓	✓	
T9	SRS Strong				✓	✓	✓
T10	INL CLSM				✓	✓	
T11	SRS Alternative 1				✓	✓	
T12	SRS Alternative 2						

*Colors key to drum location on Figure 3-2.

Table 3-2. U.S. Department of Energy Grout Formulations for 3-ft^3 Batches (Actual Batch Volume Varied)

Material Components	Savannah River Site (SRS) Strong Grout*	SRS Reducing Grout†	SRS Alternatives†		Idaho National Laboratory (INL) Heel Grout‡	INL Controlled Low Strength Material (CLSM) Grout‡	INL Pipe Grout‡
			1	2			
Portland Type I/II Cement§ (lbm‖)	61.1	8.4	33.7	20.6	25.2	33.3	74.8
Silica Sand¶ ASTM C–33 (lbm)	253.9	254.3	157.1	104.7	276.3	209.6	—
Ground Granulated Blast-Furnace Slag Cement Grade 120# (lbm)	—	22.4	33.7	28.0	38.9	—	—
Fly Ash Class F** (lbm)	—	41.1	87.9	93.5	13.1	22.2	177.6
No. 8 Aggregate Pea Gravel (lbm)	—	—	—	176.9	—	—	—
Water (gal††)	5.2	6.7	7.0	6.7	4.1	4.2	10.8
RECOVER Hydration Stabilizer‡‡ (ml§§)	—	—	32.6	32.6	—	—	—
ADVA 380 High-Range Water Reducer‡‡ (ml)	302.6	272.0	161.5	161.5	80.5	312.3	195.5
Sodium Thiosulfate, Pentahydrate‖‖ (gm ¶¶)	—	90.7	90.7	90.7	—	—	—
Viscofier Kelco-crete®## (gm)	12.0	30.6	23.8	23.8	—	—	—

*Langton, C.A., A. Ganguly, C.A. Bookhammer, M. Koval, and W.L. Mhyre. "Grout Formulations and Properties for Tank Farm Closure (U)." WSRC-STI-2007-00641 Revision 0. Aiken, South Carolina: Washington Savannah River Company. 2007.
†Langton, C.A. and J.R. Cook. "Recent Progress in DOE Waste Tank Closure." Waste Management Symposium 2008. February 24–28, 2008. Phoenix, Arizona. Table I. WSRC–STI–2007–00686. Aiken, South Carolina: Washington Savannah River Company.
‡Langton, C.A. and J.R. Cook. "Recent Progress in DOE Waste Tank Closure." Waste Management Symposium 2008, Phoenix, Arizona, February 24–28, 2008. Table III. WSRC–STI–2007–00686. Aiken, South Carolina: Washington Savannah River Company.
§Alamo Concrete Products, Supplier
‖1 lbm = 0.4536 kg
¶U.S. Silica, Supplier
#Labarge North America, Supplier
**Boral Material Technologies, Supplier
††1 U.S. liquid gal = 0.003 785 m^3
‡‡W.R. Grace Concrete Products, Supplier
§§1 ml = 0.061 02 in^3
‖‖Thermo Fisher Scientific Inc., Supplier
¶¶1 gm = 2.205 $\times 10^{-3}$ lbm
##CP Kelco, Supplier

insulation after the final lift was poured and had begun to set (Table 3-1). Grout in drums with insulated tops represent grout near the center and base of an NDAA waste tank, and drums with open tops represents grout at and near the top of an NDAA waste tank. Each test specimen was instrumented with nine thermocouple sensors (Figure 3-2) to monitor the transient temperature distribution and evolution during curing. Resulting data are discussed in Section 3.2.

The grout batches used to prepare the drum grout specimens were mixed in a 0.17-m^3 [6-ft^3] drum-type Kushlan concrete mixer. A 0.085-m^3 [3-ft^3] batch size was selected to be sufficient to fill one-third of a drum in an approximately 25-cm [10-in] lift while also providing enough material for a small archival sample. This batch size was also determined to be an appropriate size for efficient mixing in the concrete mixer. The masses and volumes of the grout ingredients were determined by proportionately adjusting the quantities DOE reported for specific grout formulations[1] (Table 3-2) to meet a final volume of approximately 0.085 m^3 [3 ft^3]. Each grout batch varied slightly in material quantities from the nominal formulation recipe and varied more significantly in the water quantity; specifically, to meet the flowability specifications, we had a lower water-to-cement ratio in almost every case (Appendix A). Grout batch details are provided in Appendix A and, with the exception of INL controlled low strength material (CLSM) batches, summary statistics are provided in Table 3-3. In the exceptional case of the INL CLSM Grout, the nominal formulation did not yield 0.085 m^3 [3 ft^3] and was insufficient to fill the drums to planned levels. To correct this situation, the nominal formulation quantities for INL CLSM Grout were adjusted proportionately upward several times to obtain the required volume and therefore do not lend themselves to provision of summary statistics.

The ingredients for the grout formulations were prepared by preweighing the solid materials and additives. During the mixing of all grouts, a portion of the water specified in the nominal grout formulation was withheld and only added as necessary until the batch achieved the desired flow characteristic {measured according to ASTM 6103-4 to be at least 25 cm [10.0 in] in diameter for all SRS grouts and the INL CLSM Grout, and measured according to slump flow test ASTM C-1161 to be 15 to 28 cm [6 to 11 in] in diameter for the INL Heel Grout}. Although the desired flow for the SRS grouts and the INL CLSM Grout was at least 28 cm [11.0 in] based on Langton, et al. (2007), experience with the various grout mixes indicated that solid–liquid segregation sometimes occurred before the flow characteristic reached 28 cm [11.0 in]. If an SRS or INL CLSM grout mix either flowed to 28 cm [11.0 in] or else flowed to at least 25 cm [10.0 in] and appeared to be on the verge of solid–liquid segregation, water addition was stopped. Grout was then transferred from the mixer to the drums in buckets at approximately 9.5 L [2.5 gal] per bucket. The development of drum grout specimen T9 is documented in Figure 3-3.

Mixing SRS Alternative 1 Grout was particularly difficult because this formula tended to ball up in dry clods when adding the fines, like certain cake batters. Despite including significant quantities of fly ash and blast furnace slag cement in their formulas, the SRS Alternative grouts had fairly rapid thermal hydration responses in comparison to the delayed response of SRS Reducing Grout. The lower maximum temperature associated with SRS Alternative 2 Grout is attributed to the fact that SRS Alternative 2 Grout had pea gravel as a large-volume additional ingredient, and pea gravel is nonreactive. Both SRS Alternative grouts set up and hardened overnight.

[1]DOE grout formulations were expressed in terms of either 1 cubic yard or 1 cubic meter batches.

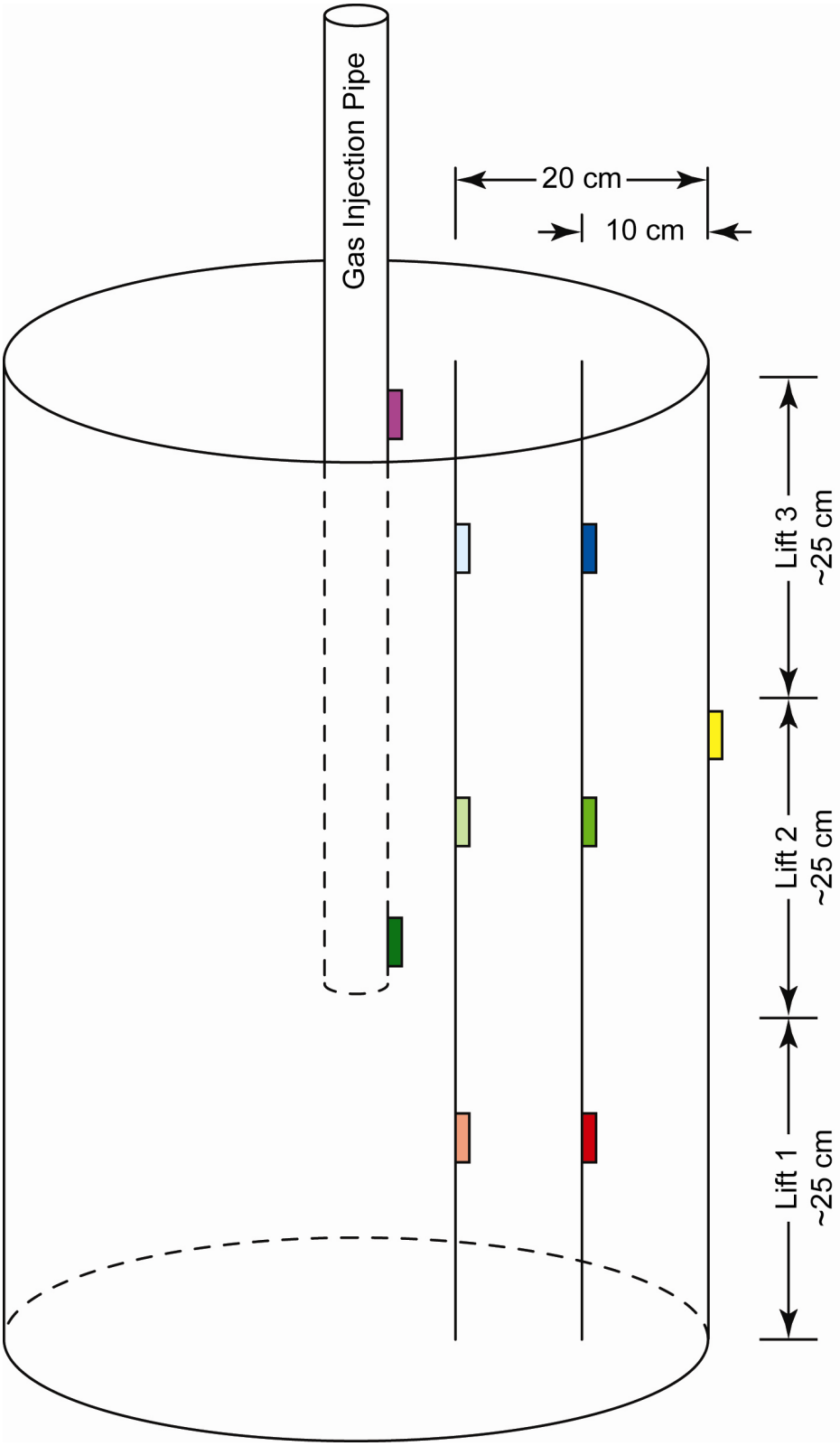

Figure 3-2. Relative Placement of Thermocouples in a Typical Drum Grout Specimen. Drawing Not to Scale. Thermocouple Colors Key to Temperature Curves in Section 3.2. Note: 1 in = 2.54 cm.

Table 3-3. Summary Statistics of Grout Batch Ingredient Quantities and Resulting Bulk Densities for Drum-Scale Specimens						
Savannah River Site (SRS) Reducing* Grout Materials for 3-ft^3 Batches	**Nominal Quantity**	**Min**	**Max**	**Mean**	**Standard Deviation**	**Units**
Portland Type I/II Cement	8.4	8.4	8.9	8.8	0.2	lbm
Silica Sand ASTM C–33	254.3	254.4	256.0	254.8	0.8	lbm
Ground Granulated Blast-Furnace Slag Cement Grade 120 ASTM C989	22.4	22.4	22.6	22.5	0.1	lbm
Fly Ash Class F	41.1	41.1	41.2	41.2	0.1	lbm
Water	6.7	4.9	5.2	5.0	0.1	gal
ADVA 380 High-Range Water Reducer	272.0	270.0	270.0	270.0	0.0	ml
Viscofier Kelco-crete®	30.6	29.5	30.2	29.9	0.3	gm
Sodium Thiosulfate, Pentahydrate	102.1	90.7	92.1	91.1	0.7	gm
Bulk Density	—	2115	2169	2138	25	kg/m^3
SRS Strong† Grout Materials for 3-ft^3 Batches	**Nominal Quantity**	**Min**	**Max**	**Mean**	**Standard Deviation**	**Units**
Portland Type I/II Cement	61.1	60.4	61.5	61.3	0.4	lbm
Silica Sand ASTM C–33	253.9	253.8	254.0	254.0	0.1	lbm
Water	5.2	4.9	5.6	5.2	0.2	gal
ADVA 380 High-Range Water Reducer	302.6	302.0	303.0	302.1	0.4	ml
Viscofier Kelco-crete®	12.0	12.0	12.3	12.2	0.1	gm
Bulk Density	—	2149	2210	2193	20	kg/m^3
SRS Alternative 1‡ Grout Materials for 3-ft^3 Batches	**Nominal Quantity**	**Min**	**Max**	**Mean**	**Standard Deviation**	**Units**
Portland Type I/II Cement	33.7	33.6	34.1	33.8	0.2	lbm
Silica Sand ASTM C–33	157.1	157.0	157.2	157.2	0.1	lbm
Ground Granulated Blast-Furnace Slag Cement Grade 120 ASTM C989	33.7	33.6	35.4	34.0	0.7	lbm
Fly Ash Class F	87.9	86.4	88.0	87.7	0.6	lbm
Water	7.0	6.0	6.6	6.3	0.3	gal
ADVA 380 High-Range Water Reducer	161.5	162.0	162.0	162.0	0.0	ml
Viscofier Kelco-crete®	23.8	23.8	23.8	23.8	0.0	gm
Sodium Thiosulfate, Pentahydrate	102.1	90.7	90.7	90.7	0.0	gm
RECOVER Hydration Stabilizer	32.6	33.0	33.0	33.0	0.0	ml
Bulk Density	—	2048	2080	2061	13	kg/m^3
SRS Alternative 2§ Grout Materials for 3-ft^3 Batches	**Nominal Quantity**	**Min**	**Max**	**Mean**	**Standard Deviation**	**Units**
Portland Type I/II Cement	20.6	21.1	21.1	21.1	0.0	lbm
No. 8 Aggregate Pea Gravel	176.9	176.8	177.0	177.0	0.1	lbm
Silica Sand ASTM C–33	104.7	104.6	104.8	104.8	0.1	lbm
Ground Granulated Blast-Furnace Slag Cement Grade 120 ASTM C989	28.0	28.0	28.0	28.0	0.0	lbm
Fly Ash Class F	93.5	93.4	93.6	93.6	0.1	lbm
Water	6.7	5.6	6.3	5.9	0.3	gal
ADVA 380 High-Range Water Reducer	161.5	162.0	162.0	162.0	0.0	ml
Viscofier Kelco-crete®	23.8	23.8	23.8	23.8	0.0	gm
Sodium Thiosulfate, Pentahydrate	102.1	90.7	90.7	90.7	0.0	gm
RECOVER Hydration Stabilizer	32.6	33.0	33.0	33.0	0.0	ml
Bulk Density	—	2043	2201	2143	59	kg/m^3

Table 3-3. Summary Statistics of Grout Batch Ingredient Quantities and Resulting Bulk Densities for Drum-Scale Specimens (continued)						
Idaho National Laboratory (INL) Heel‖ Grout Materials for 3-ft^3 Batches	**Nominal Quantity**	**Min**	**Max**	**Mean**	**Standard Deviation**	**Units**
Portland Type I/II Cement	25.2	25.2	25.2	25.2	0.0	lbm
Silica Sand ASTM C–33	276.3	276.4	276.4	276.4	0.0	lbm
Ground Granulated Blast-Furnace Slag Cement Grade 120 ASTM C989	38.9	39.0	39.0	39.0	0.0	lbm
Fly Ash Class F	13.1	13.2	13.2	13.2	0.0	lbm
Water	4.1	4.4	4.6	4.5	0.1	gal
ADVA 380 High-Range Water Reducer	80.5	81.0	111.0	100.1	13.2	ml
Bulk Density	—	2016	2196	2087	77	kg/m^3

*Sample Size n = 4
†Sample Size n = 8
‡Sample Size n = 6
§Sample Size n = 6
‖Sample Size n = 4

The INL grouts caused several difficulties. Unlike all other grout formulas, the INL Heel Grout batches were tested for their flow characteristics using slump flow test ASTM C–1161, as described in CH2M WG Idaho, LLC (2007). This specification called for slump flow of 15 to 28 cm [6 to 11 in] in diameter. DOE's grout formulas for INL Heel Grout are ambiguous in that two descriptions of this grout formula exhibited two different quantities for water and high-range water reducer (Langton and Cook, 2008; CH2M WG Idaho, LLC, 2007). Specifically, the quantity of water is given as either 22.3 L [5.9 gal] or as 15.5 L [4.1 gal], and the quantity of high-range water reducer is given as either 262.9 ml [8.9 oz] or as 80.5 ml [2.7 oz] per 0.085-m^3 [3-ft^3] batch. The specifications in CH2M WG Idaho, LLC (2007) allow the water and high-range water reducer quantities to be adjusted to meet the slump specifications. These formulas did not produce a grout that would meet the slump flow specification. Rather, water and high-range water reducer (ADVA 380) quantities actually used were in between these two limits (see Table 3-3) to achieve a self-consolidating texture with the desired slump flow. Meeting this slump flow specification resulted in a grout that was very thick (and as we shall see in Section 3.3, also very permeable). INL Heel Grout hardened significantly throughout the workday hours each day a lift was emplaced.

Despite concerted efforts to prevent solid–liquid segregation, the formula for INL CLSM Grout produced a grout prone to segregation. Specifically, while in the mixer and during testing of the flow characteristics, INL CLSM Grout never seemed on the verge of segregation as some other formulas had, but when mixing stopped and this grout was poured into a drum or archival sample container, solids and water would immediately segregate, leaving standing water on the surface of each lift.

Archival samples from each grout batch were poured into 10-cm-diameter, 20-cm-high [4-in-diameter, 8-in-high] plastic, lidded cylindrical molds. The bulk density of these archived samples was later determined after the grouts had begun to set. From the measured sample height, h, and the constant container radius, r, the sample volume was calculated using the formula $\pi r^2 h$. The samples were measured on a scale to determine their mass (tared for the mold mass), then the grout mass was divided by the sample volume to obtain the sample bulk density. With the exception of INL CLSM Grout, bulk density summary statistics are also presented in Table 3-3. The mean bulk density of INL CLSM Grout was 2261.6 ± 16.5 kg/m^3 [141.2 ± 1 lbm/ft^3].

Figure 3-3. Pictorial Overview of Preparation of Drum Grout Specimen T9

3.1.2 Thermal Hydration and Drying Shrinkage Specimen

To investigate hydration and drying shrinkage effects, a single sector of a circle (i.e., pie-slice-shaped) test specimen was constructed. The sector has a 30° angle and 3-m [10-ft] radius (i.e., ¼-scale relative to a typical NDAA waste tank; see Figures 2-1 and 3-1) and is 0.9 m [3 ft] high. The specimen was designed and developed to represent conditions near the base of an NDAA tank where residual radioactive material may be present.

The radii (sides) of the sector, which were constructed of plywood and two-by-four lumber, were insulated to simulate the lateral heat flow boundary conditions in a generic NDAA tank. The arc of the sector, which was made of steel plate, was left without insulation so that a steep radial temperature gradient could develop, as could occur near the wall of an NDAA tank. The sector forms were separated from the concrete floor by only a thin plastic sheet to simulate heat loss through the foundation of a prototype DOE tank. A ramp and landing system were constructed from which to fill the container. The test specimen was constructed by filling the form with SRS Reducing Grout heel (Lift 1) and two SRS Strong Grout upper layers (Lifts 2 and 3). The grout was poured in approximately 25-cm [10-in] lifts over the course of 3 days to a thickness of 76 cm [30 in] to simulate the approximate rate at which grout could be emplaced in an NDAA tank. After the final lift was poured, the grout surface was covered with plastic sheeting and insulation to simulate thermal conditions that would be imposed by emplacement of additional grout in the prototype tank. The effect of the overburden pressure in an actual tank could not, of course, be represented in this experiment.

Black steel, schedule 40, 5-cm [2-in] pipes were suspended vertically inside the sector at 3 locations (Figure 3-4) and were temporarily sealed with plugs to prevent grout entry, as described previously in Section 3.1.1. The plugs were later removed to allow permeability testing. After initial permeability testing, all three pipes were filled with pipe grout and retested. The sector test specimen was instrumented with thermocouples as illustrated in Figure 3-4 to monitor temperature evolution in the grout. Temperature results are discussed in Section 3.2. Once grout curing had proceeded to the point that the internal specimen temperatures had returned to ambient conditions, the forms were removed for direct observation of grout separations and other details.

The SRS Reducing Grout and SRS Strong Grout used to develop the sector specimen were mixed in 0.17-m^3 [6-ft^3] batches in a 0.26-m^3 [9-ft^3] drum-type concrete mixer. Similarly to the drum grout specimens, the masses and volumes of the sector grout ingredient materials were determined by adjusting the quantities DOE reported for specific grout formulations (Table 3-2) to a final volume of 0.17 m^3 [6 ft^3]. The 0.17-m^3 [6-ft^3] batch size required 4 batches to complete a 25-cm [10-in] lift and provided enough material for a small archival sample. This batch size was also determined to be an appropriate size for efficient mixing in the concrete mixer. Because only a limited amount of fly ash[2] was available for use in the SRS Reducing Grout lift of the sector specimen, 3 full 0.17-m^3 [6-ft^3] batches and one short 0.10-m^3 [3.6-ft^3] batch of SRS Reducing Grout were prepared. Because these four batches together did not fully fill the intended volume of the first lift, an extra batch of SRS Strong Grout was added above the top of the SRS Reducing Grout to complete Lift 1 on the first day. Four full batches of SRS Strong Grout comprised Lift 2, poured on the second day, and four full batches of SRS Strong Grout comprised Lift 3, poured on the third day.

[2]Fly ash was provided by Boral Material Technologies, Inc. at no charge. Attempts to purchase fly ash were unsuccessful due to the relatively small quantity of fly ash required for these experiments.

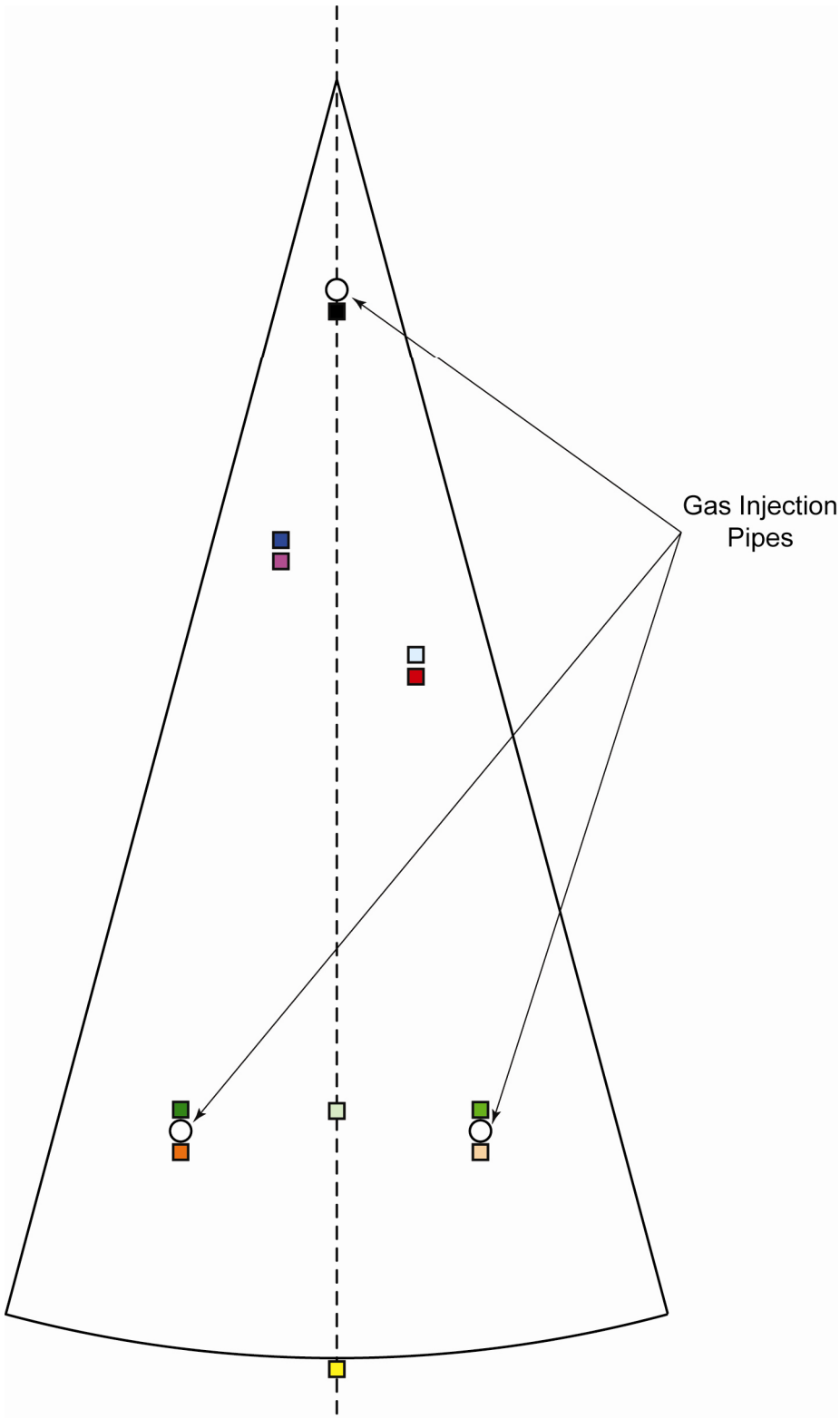

Figure 3-4. Plan View of Grout Sector Specimen Showing Approximate Locations of Gas Injection Pipes (Open Circles) and Thermocouples (Colored Squares) in Lift 1 (Orange–Red–Purple) and Lift 2 (Green–Blue–Black). Thermocouple Colors Key to Temperature Curves in Figures 9–11. Drawing Not to Scale.

Ingredients for the grout formulations were prepared by preweighing the solid materials and additives. Grout batch details are provided in Appendix A and summarized in Table 3-4. A portion of the water specified in the nominal grout formulation was withheld and only added as necessary until the batch achieved the desired flow characteristic, measured according to ASTM 6103-4, of at least 25 cm [10.0 in]. When ready, grout was transferred from the mixer to the sector specimen container in wheelbarrows via the access ramp and in buckets for more directed leveling of lifts. Emplacement of the first four grout batches was captured on a 29-minute video. Sector grout specimen development is documented in Figure 3-5. As before, archival samples from each grout batch were poured into lidded, cylindrical plastic molds. The bulk density of these archived samples was later determined after the grouts had begun to set. Summary statistics for the bulk densities are also presented in Table 3-4.

Table 3-4. Summary Statistics of Grout Batch Ingredient Quantities and Resulting Bulk Densities for ¼-Scale Sector Specimen

Savannah River Site (SRS) Reducing* Grout Materials for 6-ft^3 Batches	Nominal Quantity	Min	Max	Mean	Standard Deviation	Units
Portland Type I/II Cement	16.8	18.0	18.0	18.0	0.0	lbm
Silica Sand ASTM C–33	508.6	508.6	508.6	508.6	0.0	lbm
Ground Granulated Blast-Furnace Slag Cement Grade 120 ASTM C989	44.9	45.0	45.0	45.0	0.0	lbm
Fly Ash Class F	82.3	82.2	82.4	82.3	0.1	lbm
Water	13.5	8.8	9.8	9.3	0.5	gal
ADVA 380 High-Range Water Reducer	544.0	544.0	544.0	544.0	0.0	ml
Viscofier Kelco-crete®	61.2	61.2	61.2	61.2	0.0	gm
Sodium Thiosulfate, Pentahydrate	204.1	181.4	181.4	181.4	0.0	gm
Bulk Density	—	1957	2122	2024	87	kg/m^3
SRS Reducing† Grout Materials for Single 3.6-ft^3 Batch	**Nominal Quantity**	**Quantity Used/Measured**				**Units**
Portland Type I/II Cement	10.1	10.7				lbm
Silica Sand ASTM C–33	305.3	305.9				lbm
Ground Granulated Blast-Furnace Slag Cement Grade 120 ASTM C989	26.9	27.0				lbm
Fly Ash Class F	49.4	49.4				lbm
Water	8.1	5.6				gal
ADVA 380 High-Range Water Reducer	326.4	326.0				ml
Viscofier Kelco-crete®	36.7	36.7				gm
Sodium Thiosulfate, Pentahydrate	122.5	122.5				gm
Bulk Density	—	1999				kg/m^3
SRS Strong‡ Grout Materials for 6-ft^3 Batches	**Nominal Quantity**	**Min**	**Max**	**Mean**	**Standard Deviation**	**Units**
Portland Type I/II Cement	122.2	122.7	122.7	122.7	0.0	lbm
Silica Sand ASTM C–33	507.8	507.8	508.4	507.9	0.2	lbm
Water	10.4	9.8	11.3	10.5	0.4	gal
ADVA 380 High-Range Water Reducer	605.2	605.2	605.2	605.2	0.0	ml
Viscofier Kelco-crete®	24.0	24.0	24.0	24.0	0.0	gm
Bulk Density	—	1981	2076	2055	60	kg/m^3

*Sample Size n = 3
†Sample Size n = 1
‡Sample Size n = 9

Figure 3.5. Pictorial Overview of Preparation of Sector Grout Specimen

3.1.3 Pipe Grout Specimens

To determine whether internal pipe annuli develop when tank fixtures and pipes are grouted, one batch of INL Pipe Grout was prepared to seal six of the black steel, schedule 40, 5-cm [2-in] pipes inside the drum grout specimens and all three of the black steel pipes inside the sector grout specimen. Pipes selected for this experiment (Table 2-1) were based upon results of initial gas injection tests (discussed in Section 3.3.3).

This final grout batch required a final shipment of fly ash; thus the ingredient quantities for INL Pipe Grout were scaled for a 0.02-m^3 [0.8-ft^3] batch to be appropriate for the available mass of fly ash. Grout batch details are provided in Appendix A. Solid materials and additives were preweighed, and then the batch was mixed manually in a wheel barrow. A portion of the water specified in the grout formulation was withheld and only added as necessary to incorporate the entirety of the fly ash. Grout flowability was checked as before, using the procedure specified in ASTM 6103-4.

3.2 Thermal Evolution of Grout Monolith Specimens

This section presents observations and interpretations related to the temperature evolution of drum and sector grout specimens. Thermal evolution data were collected to inform future assessments of the effects of temperature on the properties of grout, particularly the development of fast pathways such as cracks and annuli, in full-scale grout emplacements. Temperature evolution of mesoscale specimens was primarily a function of heat and rates of hydration of pozzolanic materials (Portland cement, blast–furnace slag cement, and fly ash) used in the grout formulations and secondarily a function of conductive heat transfer between warm, newly hydrated grout lifts and cooler, newly emplaced grout lifts above, or cooler, older grout lifts below. The time interval between grout lift emplacements and the presence or absence of insulated topcovers also played roles.

3.2.1 Thermal Expansion and Contraction Specimens

Thermal evolution of the drum grout specimens is illustrated in Figures 3-6 through 3-8. SRS Strong Grout displayed the most rapid and strongest thermal hydration response, as shown in Figure 3-6a. Peak SRS Strong Grout temperatures were in the range of 50 to 55 °C [122 to 131 °F] and were matched only by peak temperatures of SRS Alternative 1 Grout specimens (Figure 3-7a). All other grout specimens (SRS Reducing, SRS Alternative 2, and INL CLSM and Heel Grouts) displayed slower heating rates and peak temperatures in the range of 35 to 40 °C [95 to 104 °F]. Note that had there not been a 1- to 5-day delay in grout emplacements in the SRS Alternative grout batches (Figure 3-7); peak temperatures in these drum grout specimens may well have been higher than recorded in this experiment. The heating rate and peak temperature is positively correlated to the fraction of Portland cement relative to other pozzolanic materials (blast furnace slag cement and fly ash) and inert materials (sand and pea gravel) contained in the grout formulations. This behavior is consistent with slow rates of hydration for fly ash and blast-furnace slag cement reported by Neville (2006).

The thermal effect of placing insulated topcovers above drum grout specimens is revealed in Figures 3-6a; 3-7a,b; and 3-8a. The intent of insulating some specimens while leaving others open to the atmosphere was to replicate, as closely as possible, conditions both in the interior of a full-scale NDAA tank as well as those near the top of an NDAA tank. Insulating the tops

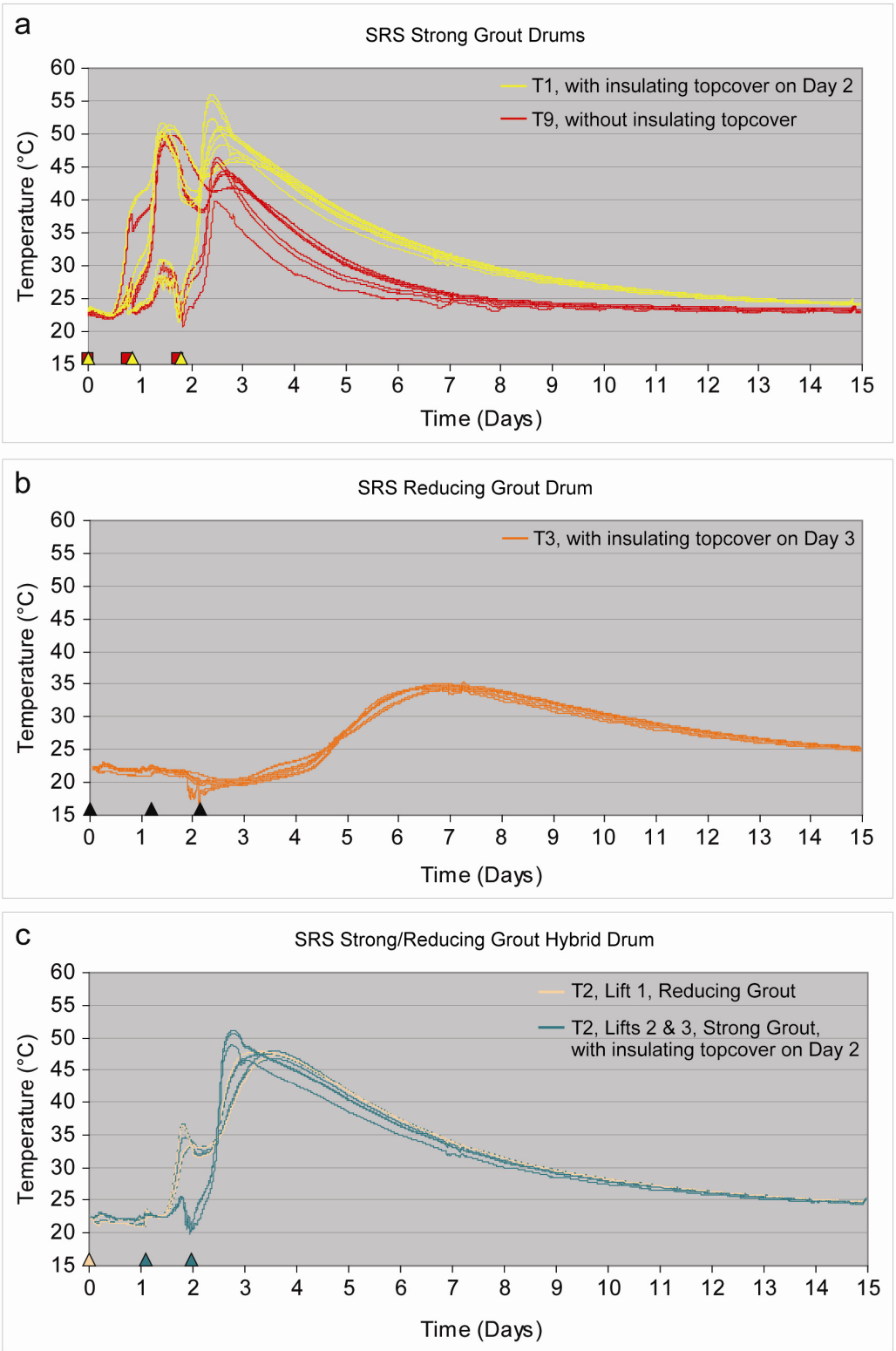

Figure 3-6. Thermal Evolution of Grout Curing in SRS Strong and Reducing Grout Drum Specimens. Temporal Variable Is Normalized to Time *t* = 0 at Emplacement of First Lift. Symbols Illustrate Timing of Lift Emplacements.

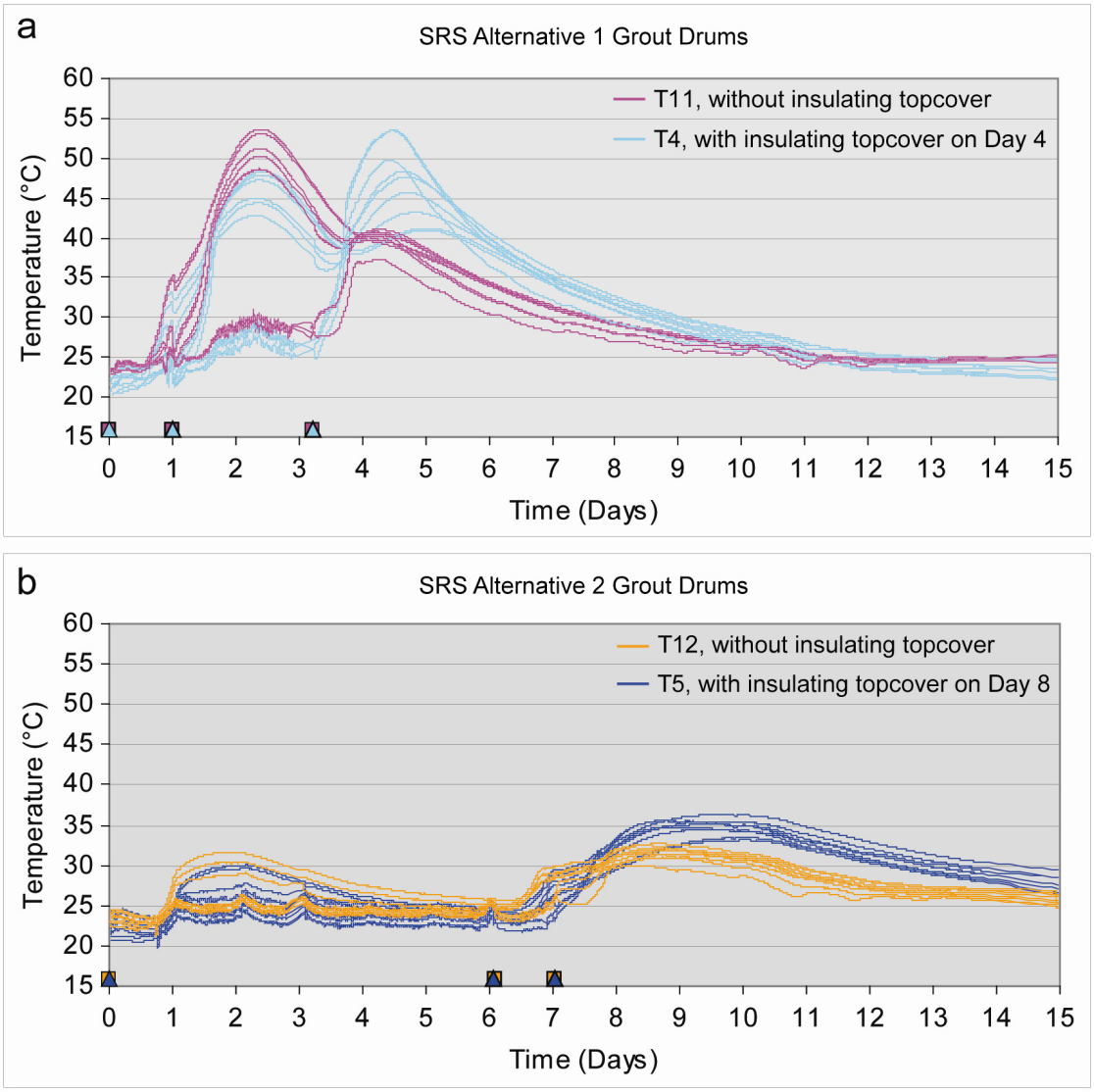

Figure 3-7. Thermal Evolution of Grout Curing in SRS Alternative Grout Drum Specimens. Temporal Variable is Normalized to Time *t* = 0 at Emplacement of First Lift. Symbols Illustrate Timing of Lift Emplacements.

of drum grout specimens reduced heat and water evaporation losses. With the exception of the SRS Alternative 1 Grout specimens (Figure 3-7a), insulation topcovers increased the peak temperature by 3 to 6 °C [5 to 11 °F] (Figures 3-6a, 3-7b, and 3-8a). Insulating SRS Alternative 1 grout drum specimen T4, however, had little effect on peak temperature compared to that attained by SRS Alternative 1 grout drum specimen T11, but dramatically affected the portion of the grout specimen that achieved the peak temperature. That is, the T4 specimen, which received a top covering of insulation on Day 4, had peak temperatures within Lift 3. Compare this to the T11 specimen, which lacked an insulation topcover and had peak temperatures in Lift 1. Lift 3 temperatures also indicate the nonintuitive result that fully insulated grout drum specimen T4 had a relatively faster rate of cooling (larger negative slope) compared to partially insulated grout drum specimen T11.

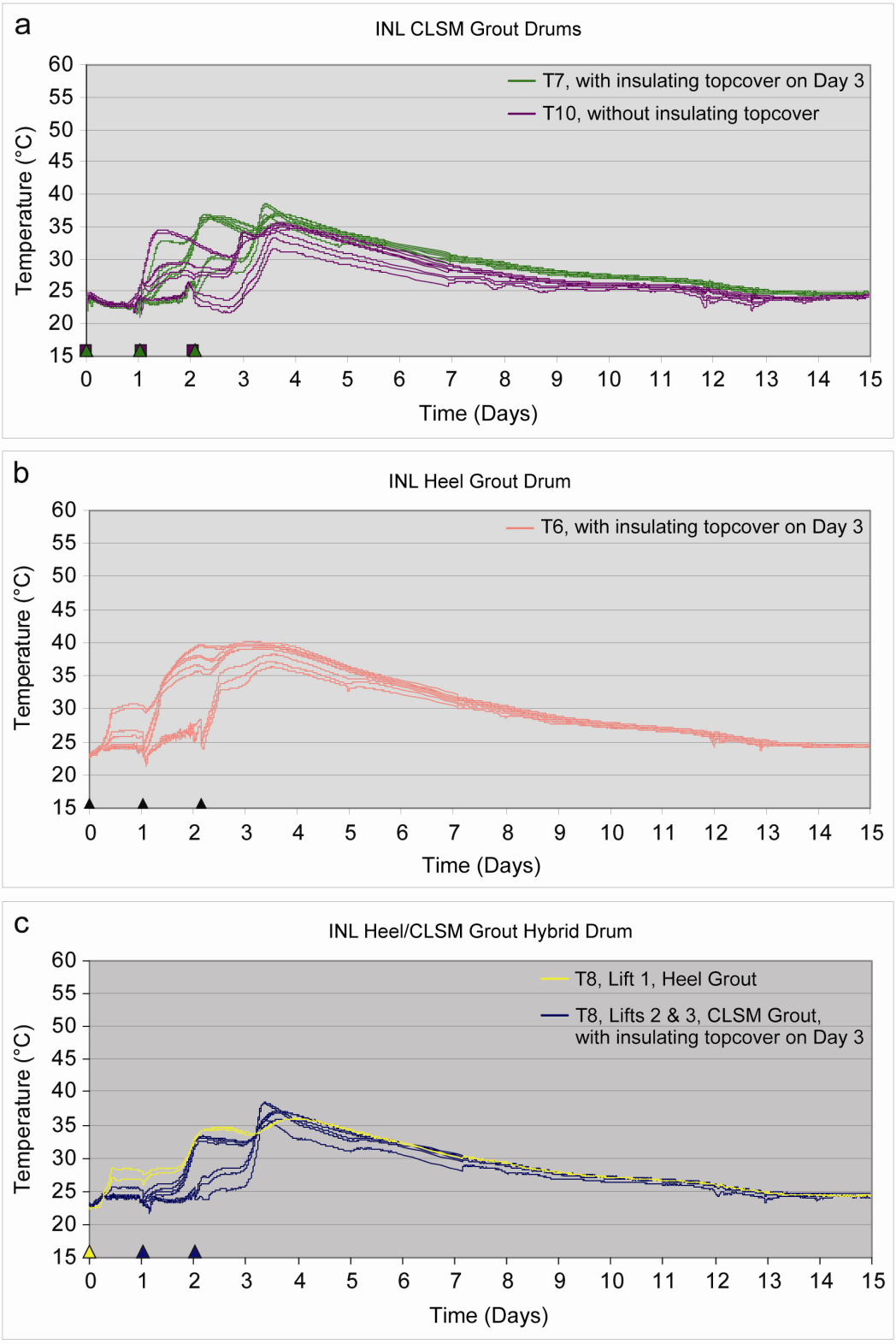

Figure 3-8. Thermal Evolution of Grout Curing in INL Grout Drum Specimens. Temporal Variable Is Normalized to Time *t* = 0 at Emplacement of First Lift. Symbols Illustrate Timing of Lift Emplacements.

Temperature gradients generated from the heat of hydration of a grout mass can create stresses that may lead to cracking if the temperature gradient is too large. Neville (2006) reports a general observation that a temperature difference greater than 20 °C [36 °F] between the interior and surface of a concrete structure can lead to cracking. This observation is based on the coefficient of thermal expansion and tensile strength of concrete. As a first step in illustrating the radial and vertical temperature differences that developed in the drum grout specimens, Figures 3-9 through 3-11 present the thermal evolution of individual thermocouples keyed to their location in each drum (Figure 3-2). Considering the temperature gradients at the point of peak temperature attainment in Lift 3, these data indicate that interior radial temperature differences within grout lifts and interior vertical temperature differences between grout lifts were less than 13 °C [23 °F] in all drum grout specimens. As a final step in illustrating vertical temperature differences between grout lifts, temperature gradients were calculated (Figure 3-12) for drum grout specimens exhibiting the largest internal temperature variation (i.e., T1, T9, T4, and T11). Negative gradients immediately following the emplacement of Lift 3 grout (Figure 3-12) indicate conductive heat transfer is carrying preexisting heat upward toward Lift 3 as its thermal hydration reactions begin, and positive gradients indicate Lift 3 heat of hydration is being carried downward to lower grout lifts by conductive heat transfer. Again, a top covering of insulation increased the temperature gradients attained by drum grout specimens T1 and T4.

Visual inspection of the exposed surfaces of the drum grout specimens did not reveal the presence of macrocracks. However, macrocracks may be present that were detected by the gas injection tests described in Section 3.3. Specifically, macrocracks may exist at grout lift contacts due to the large temperature gradient anticipated to exist in the grout near the grout mass surface, which is exposed to the significantly cooler atmosphere.

3.2.2 Thermal Hydration and Drying Shrinkage Specimen

The thermal evolution of the sector grout specimen is illustrated in Figure 3-13. Lifts 1 and 2 of the sector grout specimen were instrumented with thermocouples, but Lift 3 temperatures were not measured. The sector grout specimen contained a first lift of SRS Reducing Grout followed by two lifts of SRS Strong Grout. The temperature evolution of the sector grout specimen is similar to that of hybrid SRS Strong/Reducing drum grout specimen T2 (Figure 3-9c) in terms of heating rate and peak temperature. The maximum vertical temperature difference between Lift 1 (SRS Reducing Grout) and Lift 2 (SRS Strong Grout) was approximately 16 °C [29 °F], and the maximum lateral difference within the grout mass was approximately 5 °C [9 °F]. The maximum temperature difference between thermocouples embedded within the grout mass and the thermocouple located outside the metallic wall arc of the sector was approximately 13 °C [23 °F]. Thermally induced macrocracks were not visible on the grout surface, although separation of the grout from the gas injection pipes and radial metal boundary was visible.

3.2.3 Pipe Grout Specimens

As illustrated in Figure 3-2, each drum grout specimen has two thermocouples externally attached to the gas injection pipe. The uppermost thermocouple in each drum is located approximately 3 cm [1 in] below the Lift 3 grout surface. Temperature data obtained from these drum thermocouples were used to monitor the thermal evolution of INL Pipe Grout specimens. During the pipe grout experiment, the ambient laboratory temperature was approximately 23 °C [73 °F], insulation topcovers were no longer in place, and although sector grout specimen gas

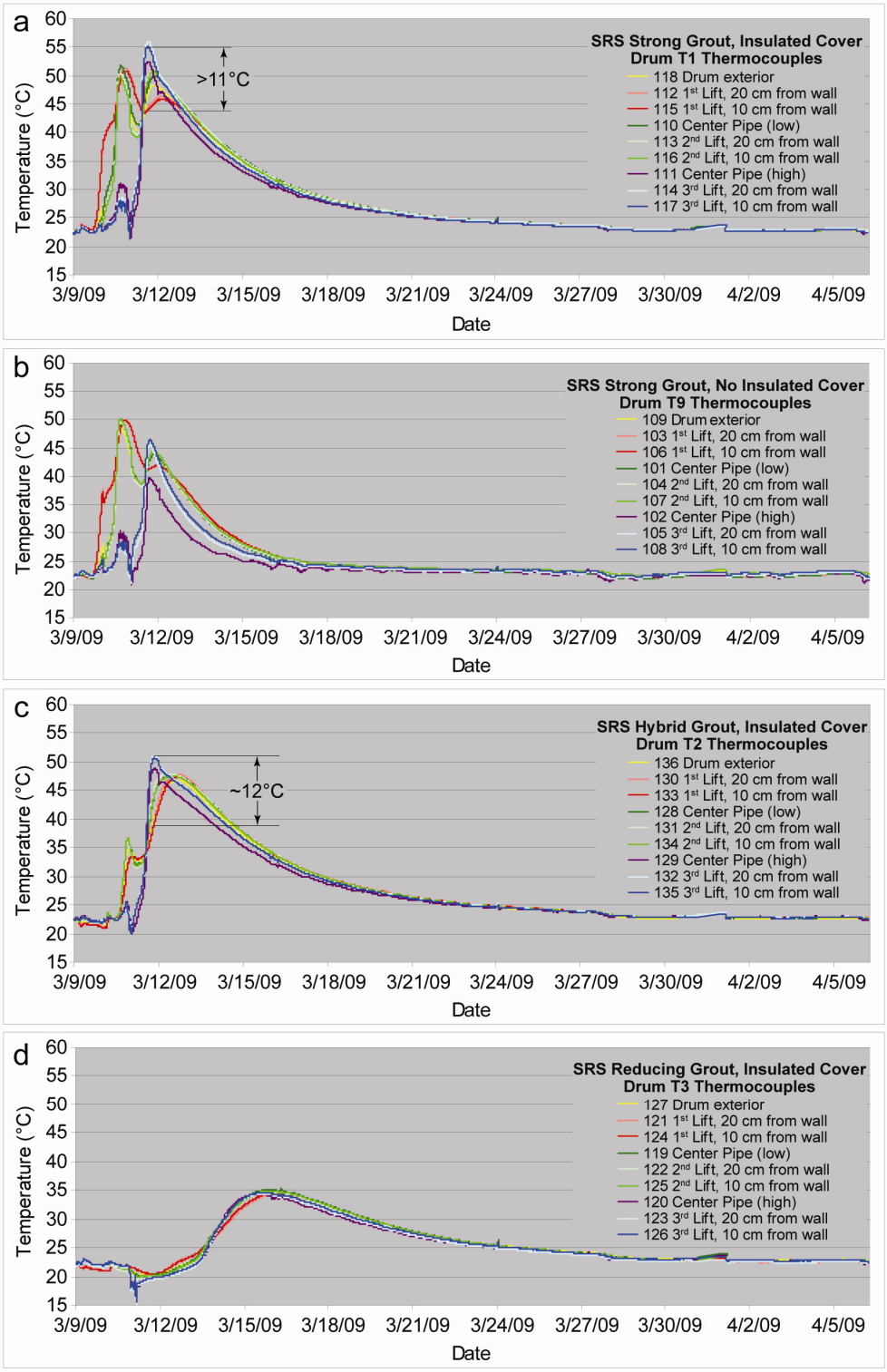

Figure 3-9. Thermocouple Response Keyed to Thermocouple Location in SRS Strong and Reducing Grout Drum Specimens. Lift 1, Lift 2, and Lift 3 Thermocouples Are Represented by the Red, Green, and Blue Color Families (Refer to Figure 3-2 for Thermocouple Location Key).

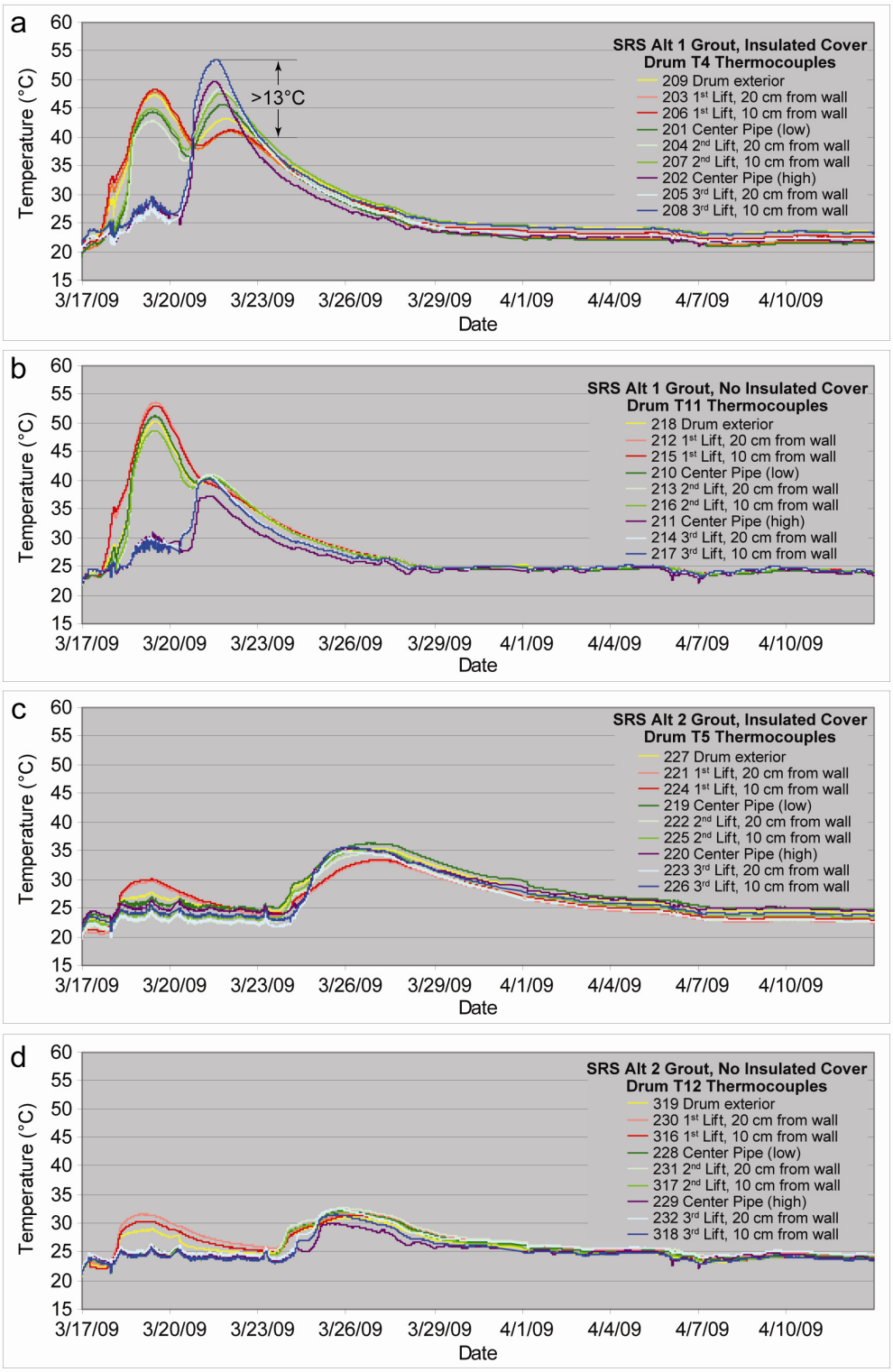

Figure 3-10. Thermocouple Response Keyed to Thermocouple Location in SRS Alternative Grout Drum Specimens. Lift 1, Lift 2, and Lift 3 Thermocouples Are Represented by the Red, Green, and Blue Color Families (Refer to Figure 3-2 for Thermocouple Location Key).

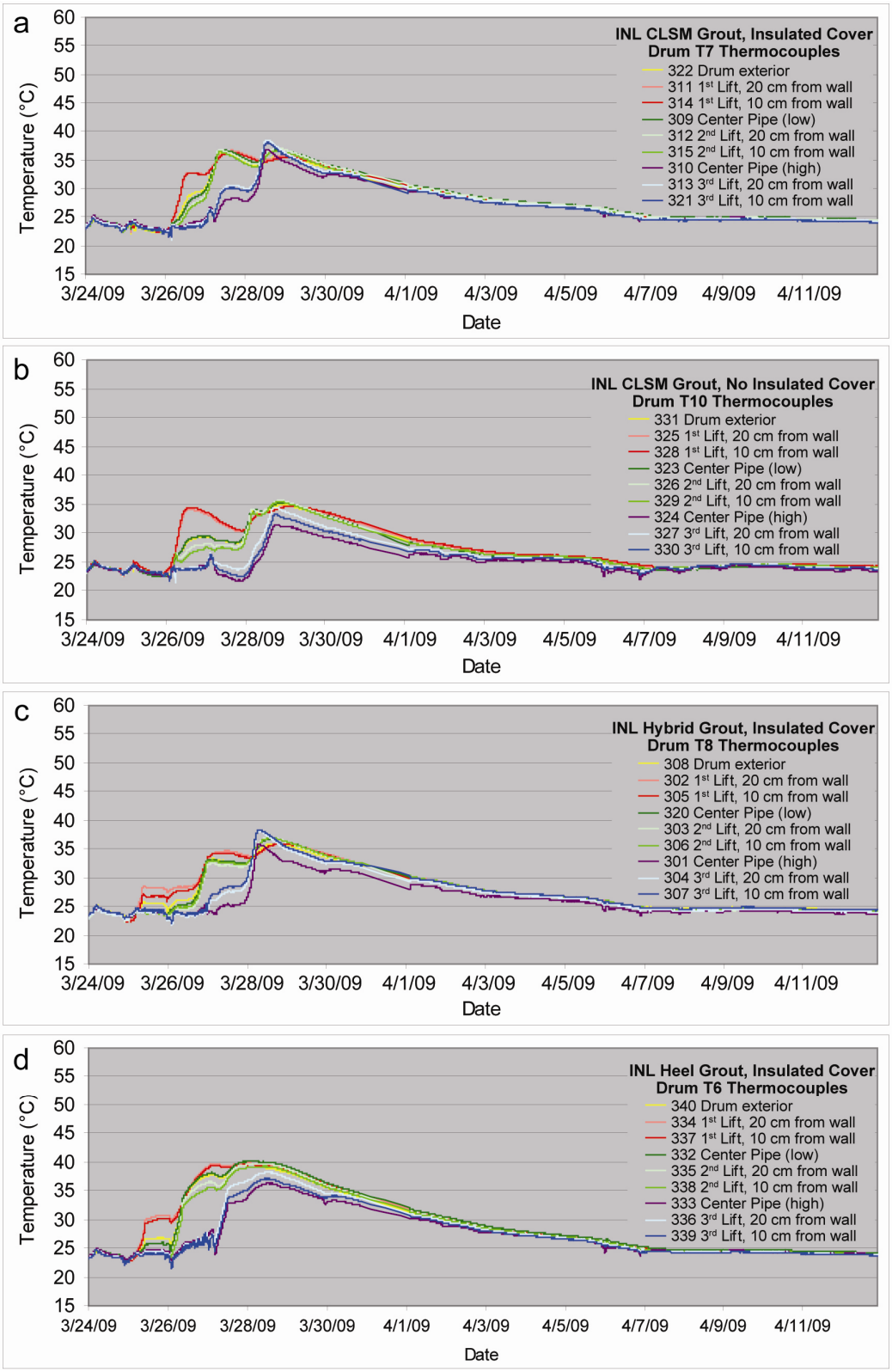

Figure 3-11. Thermocouple Response Keyed to Thermocouple Location in INL Grout Drum Specimens. Lift 1, Lift 2, and Lift 3 Thermocouples Are Represented by the Red, Green, and Blue Color Families (Refer to Figure 3-2 for Thermocouple Location Key).

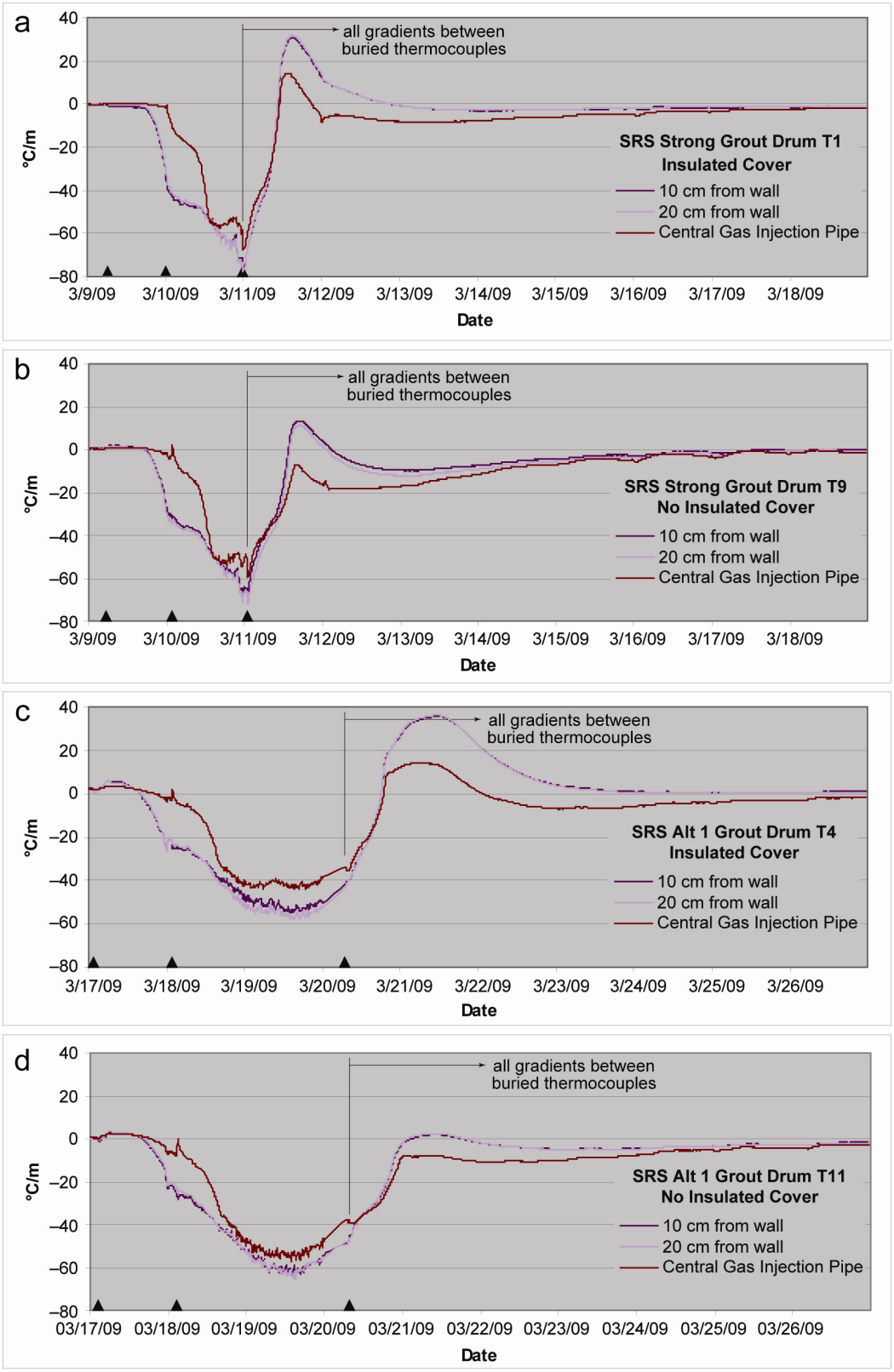

Figure 3-12. Select Temperature Gradients. Data Are From Thermocouples (Refer to Figure 3-2) on Wires in Lifts 1 and 3, and on Central Gas Injection Pipe in Lifts 2 and 3. Symbols Illustrate Timing of Lift Emplacements.

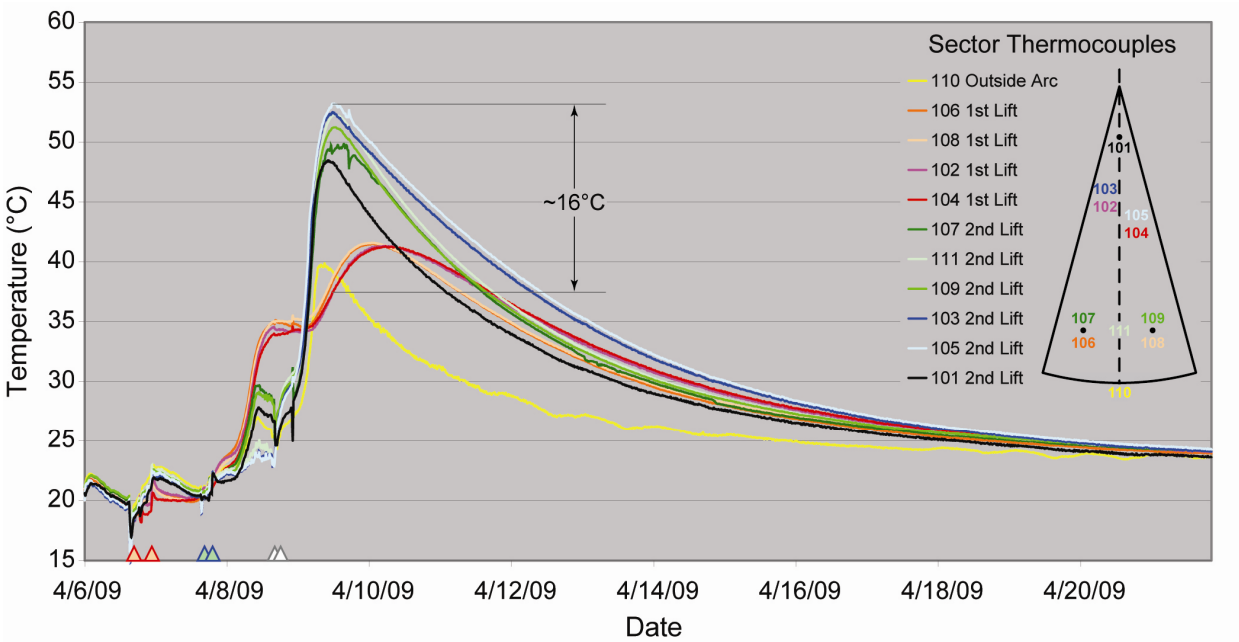

Figure 3-13. Thermal Evolution of Sector Specimen. Inset Illustrates Thermocouple and Black Steel Pipe Placement. Lift 1 and Lift 2 Temperature Data are Represented by Red–Orange and Blue–Green–Black Color Families. Symbols Illustrate Temporal Range of the Three Lift Emplacements.

injection pipes were also grouted, corresponding temperature data were not collected from sector grout specimens. Because all INL Pipe Grout specimens were prepared from the same grout batch, the temperature evolution of the sector pipe grout specimens should be similar to that monitored in the drum pipe grout specimens. Peak INL Pipe Grout temperatures (Figure 3-14) were measured in the range of 23.5 to 24.1 °C [74.3 to 75.4 °F], and approximately 2.5 and 6 days were required for the uppermost and lowermost thermocouple temperatures to return to ambient. Slight peak and near-ambient temperature variations observed for the different drum pipe grout specimens are attributed to slight variations between drums in thermocouple depth of burial and mass of emplaced pipe grout.

3.3 Analyses of Potentially Conductive Pathways in Grouted Test Specimens

Grout specimen analysis consisted of periodic visual inspection, photography, and gas injection tests. Drum grout specimens prepared with glass tubes suspended inside (specimens T9, T3, T11, T5, T8, and T10) were photographed and video-recorded using a borescope inspection system rented from Atlas Inspection Technologies. Flowability characteristics of SRS Reducing Grout were assessed during emplacement of sector grout into Lift 1; this process was video-recorded by SwRI's Media Production Services and is available for viewing on a 29-minute DVD. Grout features that may lead to potentially conductive pathways through grouted masses are discussed in Section 3.3.1; gas injection testing is described in Section 3.3.2; and analyses for preferential annular flow and bulk effective gas permeability are described and discussed in Sections 3.3.3 and 3.3.4.

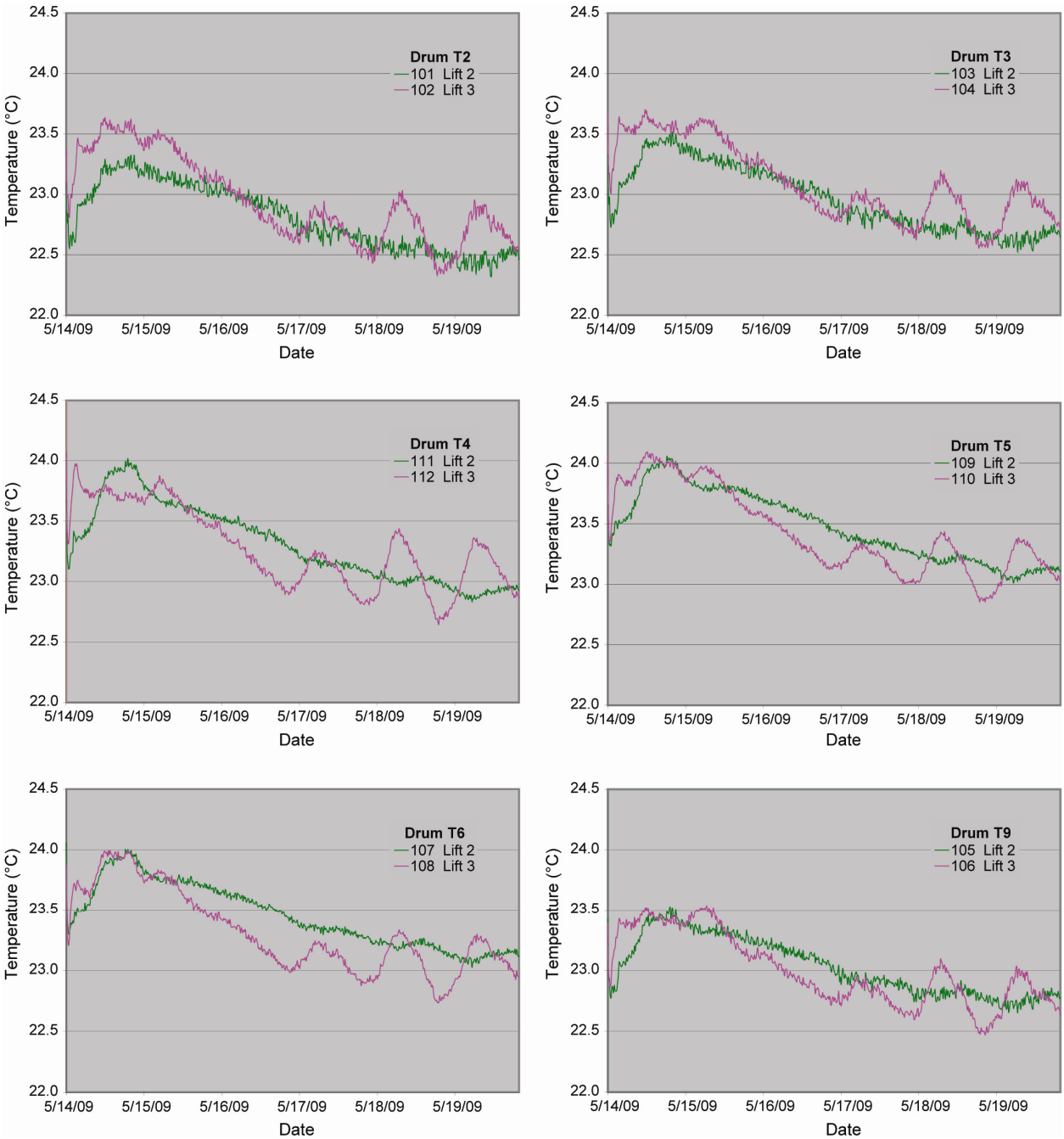

Figure 3-14. Thermal Evolution of Pipe Grout (Refer to Figure 3-2 for Thermocouple Location Key). Halfway Through the Time Series, Lift 3 Thermocouples Near the Grout Surface Strongly Indicate Ambient Diurnal Temperature Variation and Lift 2 Thermocouples at Depth Indicate a Subdued and Delayed Ambient Temperature Variation.

3.3.1 Visual Inspection and Borescopic Observations

Visual Inspection of Grout Emplacement Around Obstacles

The rheological behavior of freshly mixed grout with a water-to-cement ratio (by weight) of less than 2 (Kutzner, 1996) is similar to the behavior of fresh pahoehoe lava below the liquidus temperature; it flows to form a smooth, billowy, or ropy surface. Both are non-Newtonian fluids with rheologies that can be approximated as Bingham in nature (Kutzner, 1996; Kilburn, 1993). As grout flows around obstacles (e.g., steel pipes, copper coils, glass borescope observation tubes, and thermocouple wires), the grout mass separates on the leading edge of the obstacle and two resulting grout lobes merge together on the trailing edge. Where the two grout lobes connect, a topographically indented seam or suture forms in the wake of the obstacle (Figure 3-15a,b). As grout continues to be emplaced from a single location, this seam grows vertically to become a vertically oriented planar structure.

Poorly sorted red sand was spread thinly in the bottom of the sector specimen (above the plastic sheeting, Figure 3-5) prior to grout emplacement to evaluate the ability of SRS Reducing Grout to move particulate matter in a directed manner. Observations indicate that fine particulate matter is simply rolled over by the grout mass; only the largest particles remain mobile and move along in front of the moving grout mass.

Visual Inspection of Grout Surface Features

Grout lift surfaces were visually inspected to evaluate flowability characteristics and detect the presence of potential preferential flowpaths. Grout lift surfaces were categorized as smooth, billowy/ropy, lumpy, or as smooth (subaqueous) to rough (subaerial) (Table 3-5). Grout having relatively smooth surfaces is consistent with a very flowable cementitious material (Figure 3-15c). Grout having billowy to ropy surfaces is consistent with relatively flowable cementitious material that preserves evidence of separate grout pours from individual buckets (Figure 3-15d). Grout having rough, lumpy surfaces (Figure 3-15e) is inconsistent with flowable cementitious material and is limited to INL Heel Grout specimens (T6, and T8—Lift 1). Grout characterized as smooth (subaqueous) to rough (subaerial) is limited to INL CLSM Grout specimens (T7, T10, and T8—Lifts 2 and 3). INL CLSM Grout exhibited solid–liquid separation during emplacement, and as a result, grout solids submerged below a liquid layer cured in an utterly smooth, platy fashion, but grout solids standing above the liquid layer cured with rough patches (Figure 3-15f).

Some specimens exhibited macroscopic annuli around pipes, thermocouple wires, and drum walls, and a few cracks were observed. For example, 23 hours after SRS Reducing Grout Lift 2 was emplaced within drum grout specimen T3, the grout was observed to have pulled away from a copper coil to a significant degree (Figure 3-15g). SRS Alternative 1 and 2 Grouts and INL Heel Grout pulled away from drum walls during curing (Figure 3-15h). Visual inspection of SRS Alternative 2 drum grout lift surfaces (T5 and T12) revealed consistent formation of vesicles (Figure 3-15i). Unusual secondary surface “flow” features developed overnight at thermocouple wires in drum T12 (Figure 3-15j).

A crack of unknown depth developed overnight in INL CLSM Grout drum T7 between the gas injection pipe and a thermocouple wire (Figure 3-15k). Following grout emplacement, INL CLSM Grout surfaces were observed to form a surface rind (Figures 3-15k,l) and platy minerals

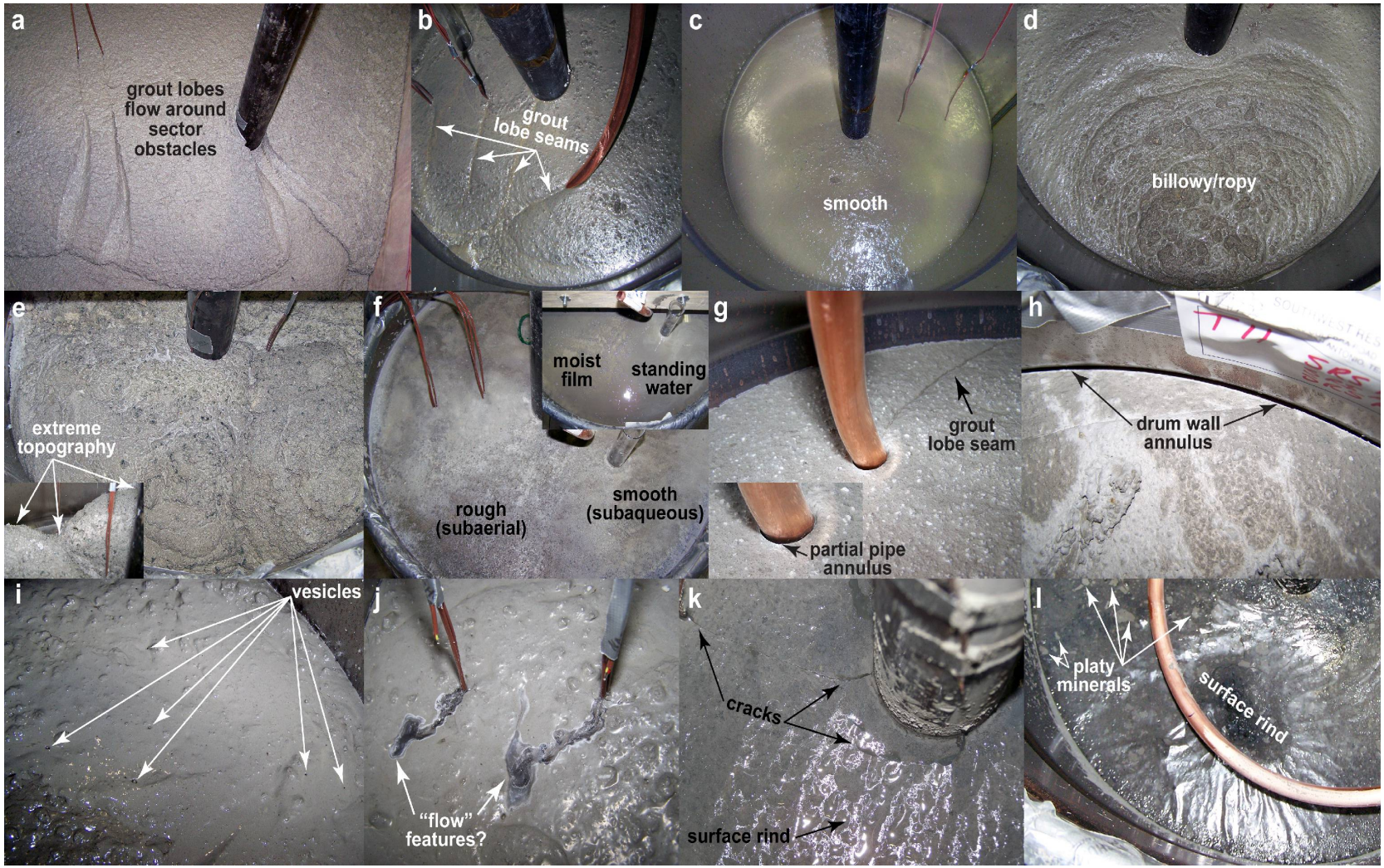

Figure 3-15. Grout Surface Features. (a) Grout Lobes Flow Around Obstacles in Sector Specimen (Lift 1). (b) Topographically Indented Seams/Sutures in Wake of Obstacles (T9, Lift 2). (c) Flowable Cementitious Material with Smooth Surface (T1, Lift 1). (d) Relatively Flowable Cementitious Material with Billowy to Ropy Surface (T1, Lift 2). (e) Nonflowable Cementitious Material with Rough, Lumpy, Extreme Topography Surface (T6, Lift 2). (f) Smooth to Rough Grout Surface Developed as a Result of Solid–Liquid Segregation (T10, Lift 3). (g) Partial Annulus Developed Around Copper Coil (T3, Lift 2). (h) Annulus Developed Around Drum Circumference (T11, Lift 3). (i) Vesicles Prolific in SRS Alternative 2 Grout (T12, Lift 2). (j) Poorly Understood Secondary Surface "Flow" Features (T12, Lift 2). (k) Crack Developed in Grout Surface (T7, Lift 1). (l) Surface Rind with Platy Minerals Develops Overnight on Grout Surface (T10, Lift 1).

Table 3-5. Drum Grout Lift Surface Texture Characteristics				
Test Specimen	**Smooth**	**Billowy/Ropy**	**Lumpy**	**Smooth (Subaqueous) to Rough (Subaerial)**
T1—Lift 1	✓			
T1—Lift 2		✓		
T1—Lift 3		✓		
T2—Lift 1		✓		
T2—Lift 2	✓			
T2—Lift 3*	?	?		
T3—Lift 1		✓		
T3—Lift 2		✓		
T3—Lift 3*	?	?		
T4—Lift 1		✓		
T4—Lift 2		✓		
T4—Lift 3		✓		
T5—Lift 1	✓			
T5—Lift 2		✓		
T5—Lift 3		✓		
T6—Lift 1			✓	
T6—Lift 2			✓	
T6—Lift 3			✓	
T7—Lift 1				✓
T7—Lift 2				✓
T7—Lift 3				✓
T8—Lift 1			✓	
T8—Lift 2				✓
T8—Lift 3				✓
T9—Lift 1	✓			
T9—Lift 2	✓			
T9—Lift 3	✓			
T10—Lift 1				✓
T10—Lift 2				✓
T10—Lift 3				✓
T11—Lift 1		✓		
T11—Lift 2		✓		
T11—Lift 3		✓		
T12—Lift 1	✓			
T12—Lift 2		✓		
T12—Lift 3	✓			

*Drum grout specimens T2 and T3 were quickly covered with insulation after final lifts were emplaced. Photographs were not collected prior to insulation being added, and the insulation flattened the grout to such an extent that it is no longer possible to tell whether the lift surface was smooth or billowy.

were frequently observed. Cracks in this grout may be shallow, limited to the thin surface rind, and related to the formation of platy minerals. Similar cracks were also observed in drum grout specimen T8, Lift 2, surrounding a thermocouple wire, and in drum grout specimen T7, Lift 2, surrounding the gas injection pipe (not shown). Well-developed cracks in the surface of T7, Lift 2, also occurred without association to internal drum fixtures.

Borescopic Observations

Features revealed by the borescopic examinations ranged from color variations (perhaps having to do with mineralogical variations) and grout texture to vesicles and large void spaces at lift interfaces. Features observed in individual drum grout specimens are described next.

SRS Strong Grout specimen T9 ranges from gray brown and coarse to gray and fine grained (Figure 3-16a). Dark-brown mottling begins at 9.5 cm [3.8 in] below the grout surface in Lift 3 and increases toward the contact between Lifts 2 and 3 until the grout is completely dark brown above the interface (Figure 3-16b). The interface between the dark-brown, coarse Lift 3 grout and the gray, fine-grained Lift 2 grout is very distinct (Figure 3-16c). The same mottling phenomenon occurs in Lift 2 and at the boundary between Lifts 1 and 2 (Figure 3-16d).

SRS Reducing Grout specimen T3 is gray and fine grained, with vesicles too small to determine shape (Figure 3-16e). Quartz particles sparkle with reflected light (Figure 3-16e,f). Black mottling increases toward the lower boundary of each lift. The lift interfaces are uneven, complex, and full of voids where grout from the lift above did not fill in topography of the lift below (Figure 3-16f).

SRS Alternative 1 Grout specimen T11 is gray and fine-grained with a broad size range of irregularly shaped vesicles. At depths of 12.4 to 13.7 cm [4.9 to 5.4 in] below the grout surface, the grout begins to appear black and mottled, and this effect increases toward the contact between Lifts 2 and 3. The black mottled regions have a distinctly vertical pattern in T11 not seen in any other drum grout (Figure 3-16g). In addition, a vertical feature is observed along the whole length of the glass borescope tube in Lift 2 (Figure 3-16h). This vertical feature is interpreted to be a planar seam or suture that developed after flowing grout split into two lobes at the leading edge of the glass tube obstacle, flowed around the obstacle, and merged together on the trailing edge of the glass tube during grout emplacement. Amoeba-shaped structures with a light center and very dark outline were observed in all three lifts of grout (Figure 3-16i). At the boundary between Lifts 1 and 2, a small 1-cm [0.4-in]-deep void was observed (Figure 3-16j). Finally, an approximately 5-cm [2-in]-deep, V-shaped feature was observed at the boundary between Lifts 1 and 2, but Lift 2 grout appears to have fully filled-in this Lift 1 crevasse.

SRS Alternative 2 Grout specimen T5 was observed to be gray and fine-grained with black mottled patches and small vesicles in all three lifts (Figure 3-16k). In the first lift, black mottling occurs between 6.3 and 8.9 cm [2.5 and 3.5 in] below the grout surface and becomes progressively more mottled until almost completely black near the contact between the lifts. The gray grout color also takes on a brown tint as the mottling increases (Figure 3-16l). At both

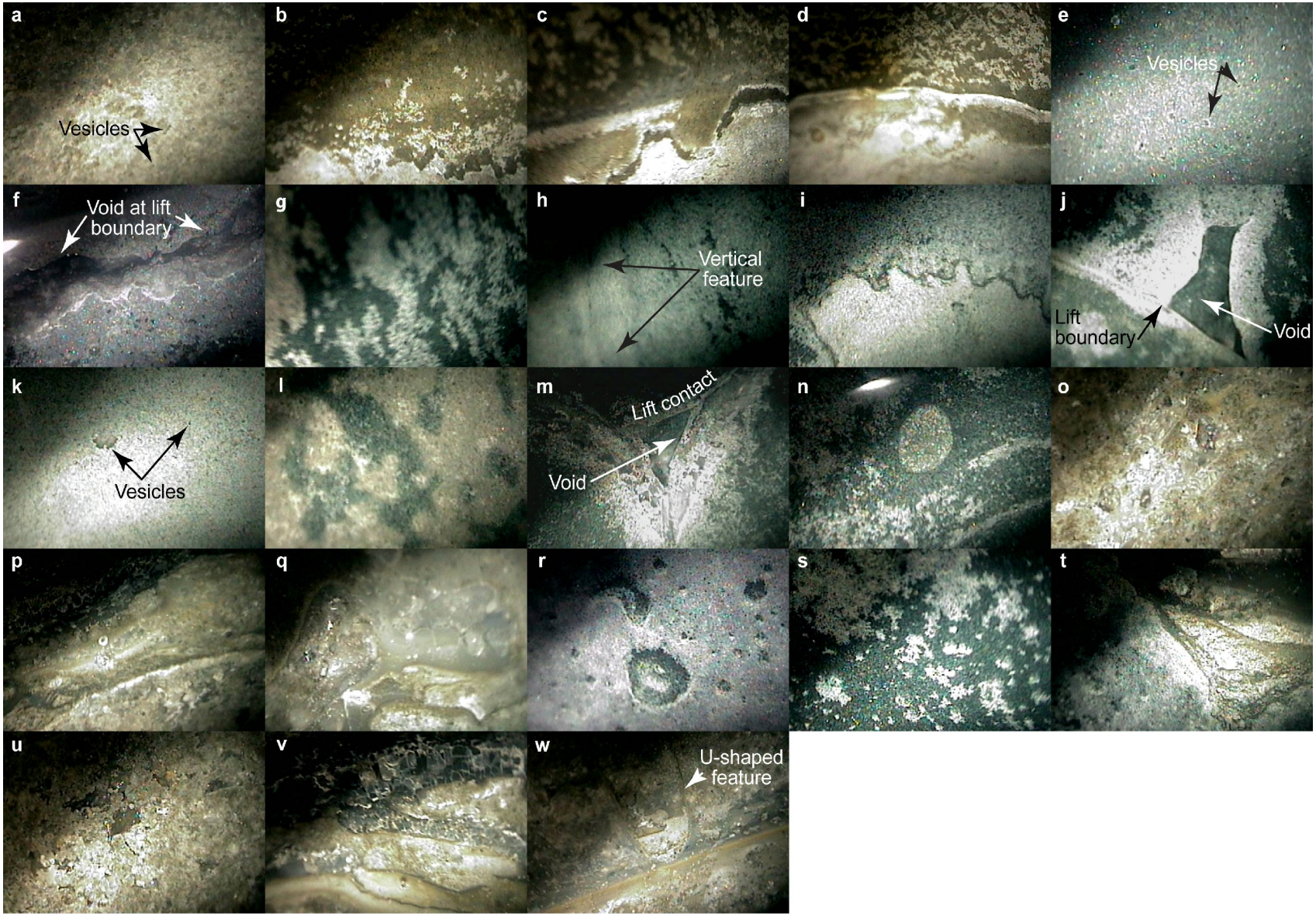

Figure 3-16. Downhole Borescope Photographs of Grout Details Discussed in Text

contacts, the grout is much lighter in color, shiny, and smoother in texture. In addition to small vesicles, larger voids were observed near the contact between Lifts 2 and 3 where Lift 3 did not completely fill in the topography of Lift 2. An approximately 2 × 2-cm [0.8 × 0.8-in], V-shaped void exists where grout from above did not flow into a crevasse in the lift below (Figure 3-16m). As in drum grout specimen T11, structures having a light center and dark outline were observed in all three lifts of specimen T5 (Figure 3-16n).

Hybrid drum grout specimen T8 contains INL Heel Grout in Lift 1 and INL CLSM Grout in Lifts 2 and 3. In general, the INL CLSM Grout is grayish brown and very shiny with vesicles scattered throughout (Figure 3-16o). The contact between Lifts 2 and 3 is thick with multiple layers of tan, dark gray, and black grout and what looks like possible void space (Figure 3-16p). This interface is uneven and convoluted with Lift 3 grout intruding into topography left by Lift 2 grout (Figure 3-16q).

INL Heel Grout is gray with many irregularly shaped vesicles in a broad range of sizes (Figure 3-16r). Black mottling appears toward the bottom of Lift 1 (Figure 3-16s). The boundary between Lift 1 and 2 is sharp, and Lift 2 INL CLSM Grout filled in the topography left behind by Lift 1 INL Heel Grout, leaving no voids to be observed by the borescope (Figure 3-16t).

INL CLSM Grout specimen T10 is grayish brown, shiny, and very rough in texture, with large, irregularly shaped vesicles (Figure 3-16u). The contact between Lifts 2 and 3 is smooth in texture, and small, whitish linear features were observed in gray layers (Figure 3-16v). This interface is composed of multiple layers of brown, gray, black, and tan grout. The contact between Lifts 1 and 2 is similar, except for the presence of a U-shaped feature in Lift 1 that is completely filled in by Lift 2 grout (Figure 3-16w). Based on photographic evidence of drum fixtures at different stages of grout emplacement, this feature may be a thin film of Lift 1 grout that splashed onto the glass tube slightly above the top surface of Lift 1, dried, and later became encased in Lift 2 grout.

3.3.2 Gas Injection Testing

Ultra-high-purity nitrogen gas was injected into the central pipe in each drum grout specimen and into all three pipes in the sector grout specimen as a test for the potential presence of cracks, lift separations, and annuli between grout and tank fixtures and sidewalls. A testing apparatus was engineered to include a pressure gauge, allowing a maximum injection gage pressure of 3.4×10^5 Pa [50 psig], and two Omega Engineering, Inc. rotameters (Models FL-110 and FL-112) capable of measuring flow rates from 0.2 to 1900 cm^3/min [7×10^{-6} to 6.6×10^{-2} ft^3/min]. A minimum of three different steady-state injection gauge pressure and corresponding flow rate data pairs were collected for each drum to assess the flow regime (i.e., Darcy, Forcheimer). Gas injection tests occurred approximately 3 weeks after the last drum grout specimen had been poured and approximately 2 weeks after the last lift in the sector specimen had been poured. The temperature in all specimens had returned to ambient by the time of the pressure testing. Grouted pipes were later tested in the same way to determine whether internal annuli had developed between the pipe grout and pipe wall.

Gas Injection Observations

After data collection, water was added to the surface of the grout specimens so that any significant gas flowing at the surface (i.e., around the injection pipe; the copper or glass tubing, if present, the thermocouple wires, and/or through cracks) could be observed as bubbles in the water. In the majority of drum grout specimens, gas mainly appeared to be flowing through an

annulus between the grout and the centrally located gas injection pipe. Gas flow through surface cracks in the grout was not observed in any specimen.

Drum grout specimen T6 presented an extreme exception to these observations. This drum contained a monofill of INL Heel Grout, which was not very flowable and developed rough surfaces between lifts. When gas was injected into this specimen, the gas emerged at an audibly high rate from an annulus between the grout and the drum wall.

3.3.3 Annular Aperture Analysis

For gas injection tests that exhibited significant flow around the injection pipe annulus, the pressure–flow rate data were analyzed using an analytic solution from Bird, et al. (1960, p. 53, Eq. 2.4–16) provided for fluid flow through an annulus. Their solution is applicable to this problem if the permeability of the grout mass can be considered negligible. The solution of Bird, et al. (1960) is

$$Q = \frac{\pi \Delta P (r+b)^4}{8\mu L}\left[(1-\kappa^4) - \frac{(1-\kappa^2)^2}{\ln(1/\kappa)}\right] \tag{3-1}$$

where

Q	—	volumetric flow rate [m^3/s]
ΔP	—	pressure difference [Pa] [newtons/m^2]
r	—	pipe radius [m]
b	—	annulus aperture [m]
μ	—	gas dynamic viscosity [kg/m·s]
L	—	length of annular space [m]

and

$$\kappa = r/(r+b) \tag{3-2}$$

This analytic solution assumes that (i) flow through the grout mass is small compared to flow through the annulus and (ii) the interior of the pipe at its base is in complete contact with the continuous annular void. All drum grout specimens, with the exceptions of T6 and T7, and all pipes in the sector grout specimen showed some evidence of annular flow around the injection pipe. Equations (3-1) and (3-2) were used to compute effective annular apertures for these specimens. These equations were implemented in a Microsoft® Excel® spreadsheet, and the Goal Seek solver tool was used to iteratively solve for the annulus aperture for each pressure–flow rate data pair.

Annular Aperture Analysis Prior to Emplacement of Pipe Grout

Annular aperture analysis results obtained prior to filling the gas injection pipes with INL Pipe Grout are summarized in Table 3-6. The column labeled Flow Behavior indicates whether the flow measured at various pressures deviated from Darcy's Law as evidenced by a nonlinear relationship between flow and pressure. The calculated apertures should be viewed as only approximate values because the assumptions on which Eqs. (3-1) and (3-2) are based may not have been fully met and could not be verified. With respect to the first assumption, the actual flow through the pipe annulus could not be measured; thus some gas may have flowed through the grout mass as well as through the pipe annulus. Based on visual observations during the test, this was probably the case for gas injection tests of drum grout specimens T1, T2, T7, and

Table 3-6. Calculated Average Annular Apertures Between Injection Pipe and Drum or Sector Grout					
Test Specimen	**Grout Formulation**			**Aperture (μm)**	**Flow Behavior**
	Lift 1	**Lift 2**	**Lift 3**		
Drum Grout Specimens					
T1	Savannah River Site (SRS) Strong			8.1	High Velocity Flow Effect
T2	SRS Reducing	SRS Strong		5.1	Borderline Darcy Flow
T3	SRS Reducing			6.8	High Velocity Flow Effect
T4	SRS Alternative 1			7.1	High Velocity Flow Effect
T5	SRS Alternative 2			8.8	High Velocity Flow Effect
T6	Idaho National Laboratory (INL) Heel			"78.0"	Darcy Flow (diffuse + annular between grout and drum wall)
T7	INL Controlled Low Strength Material (CLSM)			2.1	Darcy Flow
T8	INL Heel	INL CLSM		1.1	Undetermined
T9	SRS Strong			17.9	High Velocity Flow Effect
T10	INL CLSM			2.7	Darcy Flow
T11	SRS Alternative 1			6.2	High Velocity Flow Effect
T12	SRS Alternative 2			7.3	Darcy Flow
¼-Scale Sector Grout Specimen					
Pipe A	SRS Reducing	SRS Strong		19.7	High Velocity Flow Effect
Pipe B	SRS Reducing	SRS Strong		17.5	High Velocity Flow Effect
Pipe C	SRS Reducing	SRS Strong		13.9	Borderline Darcy Flow

T8. Visual observation of bubble evolution at the grout surface indicated that flow was relatively uniform around the pipe circumference in some tests, whereas bubbles emerged from isolated channels around the pipe in others.

With one exception, the calculated annulus apertures for the drum grout specimens are relatively consistent, ranging from 1 to 18 μm [39 to 710 μin]. INL CLSM Grout specimens developed the smallest apparent apertures, and the largest apparent aperture developed in a drum of SRS Strong Grout (Table 3-6). The 78-μm [3070-μin] "aperture" computed for drum grout specimen T6 (Table 3-6) is clearly influenced by both annular and diffuse flow through the grout based on visual and audible observation of gas emerging from an annulus between the grout and drum wall (unlike the other specimens from which gas emerged from an annulus between the grout and the gas injection pipe). The apertures computed for drum grout specimens T1, T2, and T8 may also be influenced by diffuse flow based on visual observations that gas, which emerged around the pipe, appeared to be less than the total measured gas flow rate. In the case of drum grout specimen T7, no gas flow was observed around the pipe.

The apertures computed from the sector specimen tests were consistently at the high end of the drum specimen scale, ranging from approximately 14 to 20 μm [550 to 790 μin]. The larger calculated aperture values for the sector grout specimen are consistent with visual observation of macroscopic annuli around the sector specimen gas injection pipes. The larger annuli for the sector specimen may be due to the greater potential for hydration shrinkage and thermal contraction in the sector grout specimen compared to that of the drum grout specimens due to the sector specimen's greater volume. However, note that one drum specimen of SRS Strong Grout did have an apparent aperture of this magnitude, so one cannot rule out the possibility that the grout formulation itself may have had a role in the size of the annulus that developed.

Annuli Remaining After Pipe Grout Emplacement

Based upon the initial gas injection test results, INL Pipe Grout was used to seal the gas injection pipes of drum grout specimens T2, T3, T4, T5, T6, and T9 and all three gas injection pipes in the sector grout specimen. The gas injection tests were then repeated and analyzed as noted previously. Results are presented in Table 3-7. As before, the column labeled Flow Behavior indicates whether the flow measured at various pressures deviated from Darcy's Law as evidenced by a nonlinear relationship between flow and pressure. The apertures listed in Table 3-7 were calculated using Eq. (3-1) assuming that the flow path length, *L*, was the sum of the length of pipe grout inside the pipe plus the length of grout outside the pipe. Thus, the computed apertures represent a composite of the aperture inside and outside the pipe. The calculation is only approximate, however, because it does not account for the flow direction reversal that occurs at the base of the pipe. This flow reversal could contribute to pressure loss that would cause the computed apertures to be too small. Again, the calculated apertures should be viewed as only approximate values because the assumptions on which Eqs. (3-1) and (3-2) are based may not have been fully met and could not be verified. With respect to the first assumption, the actual flow through the pipe annulus could not be measured; thus some gas may have flowed through the grout mass as well as through the pipe annulus. The calculated annular apertures for the pipe grout specimens are relatively consistent, ranging from 0 to 4.5 μm [0 to 177 μin].

3.3.4 Effective Gas Permeability Analysis and Estimates

The bulk effective gas permeability of a drum grout specimen was estimated based on the steady-state gas flow tests described in Section 3.3.2. The effective gas permeability was computed using an injection pressure–steady gas flow rate correlation developed using the numerical gas flow code BIGEM (Walter, 2005). The BIGEM code assumes ideal gas compressibility and simulates flowing gas under moderate pressure. The code was used to develop a correlation between gas flow rate and injection pressure assuming uniform flow throughout the grout matrix. This correlation was then used to compute an effective gas permeability for those drum grout specimens that displayed evidence of diffuse flow.

Drum Model

Gas flow through the drums was simulated using the two-dimensional, axisymmetric numerical model grid illustrated in Figure 3-17. The left boundary of the grid is aligned with the centerline of the injection pipe, and the first column of grid nodes is located at r = 0.0127 m [0.04167 ft]. The remainder of the grid has a constant spacing of 0.005 m [0.0164 ft] in both the radial and vertical directions. The boundary condition on the portion of the grid covered by the pipe is defined as no flow. The cell corresponding to the lower open end of the gas injection pipe has a prescribed pressure boundary condition. The boundary condition corresponding to the upper grout surface is specified as constant atmospheric pressure. The remaining boundary conditions are specified as no flow. The injection pressure in the pipe was applied to grid cells representing the injection area at the bottom of the pipe.

This numerical model was used to develop a correlation between the square of the injection pressure and steady flowrate. The correlation was of the Q_{sc} form

$$k_{eg} = S_f \frac{\mu}{\rho g} \frac{Q_{sc}}{\Delta P^2} \tag{3-3}$$

Table 3-7. Calculated Average Annular Apertures Between Idaho National Laboratory (INL) Pipe Grout and Injection Pipe					
Test Specimen	**Grout Formulation**			**Aperture (μm)**	**Flow Behavior**
	Lift 1	**Lift 2**	**Lift 3**		
Drum Grout Specimens					
T2	Savannah River Site (SRS) Reducing	SRS Strong		3.5	Indeterminate
T3	SRS Reducing			1.5	Indeterminate
T4	SRS Alternative 1			0.0	No Flow
T5	SRS Alternative 2			3.9	Darcy Flow
T6	INL Heel			0.0	No Flow
T9	SRS Strong			2.7	Darcy Flow
¼-Scale Sector Grout Specimen					
Pipe A	SRS Reducing	SRS Strong		4.5	Darcy Flow
Pipe B	SRS Reducing	SRS Strong		0.0	No Flow
Pipe C	SRS Reducing	SRS Strong		4.4	Darcy Flow

and

$$\Delta P^2 = \left(P_{ig} + P_A\right)^2 - P_A^2 \tag{3-4}$$

where

k_{eg} — effective gas permeability (m^2)
S_f — slope of the regression between ΔP^2 and Q_{sc} [$Pa^2 \cdot m \cdot min/ml \cdot s$]
ρ — gas density [kg/m^3]
g — gravitational acceleration [9.8 m/s^2]
Q_{sc} — gas flow rate at standard conditions [cm^3/min]
P_A — atmospheric pressure [Pa]
P_{ig} — injection gage pressure [Pa]

The effective gas permeability is related to the effective gas conductivity, K_{eg} (m/s), by

$$k_{eg} = \frac{\mu}{\rho g} K_{eg} \tag{3-5}$$

The BIGEM code computes effective gas conductivity using the Brooks–Corey relationship between saturated hydraulic conductivity, porosity, and water content (Brooks and Corey, 1966). Because the water content of the grout was not known at the time of the gas injection tests and because the parameters required to relate the gas permeability to the saturated hydraulic conductivity for the grout have not been determined, the Brooks–Corey input parameters were simply adjusted so that the gas conductivity would equal the saturated hydraulic conductivity used in the input file. The actual porosity and water content specified in the simulation did not affect the steady-state flowrate and pressure calculations. Other parameters required for the simulations were

- Ambient temperature (25 °C)
- Nitrogen gas dynamic viscosity at 25 °C (i.e., 1.76×10^{-5} Pa·s)
- Nitrogen gas molecular weight (28 g/mol)

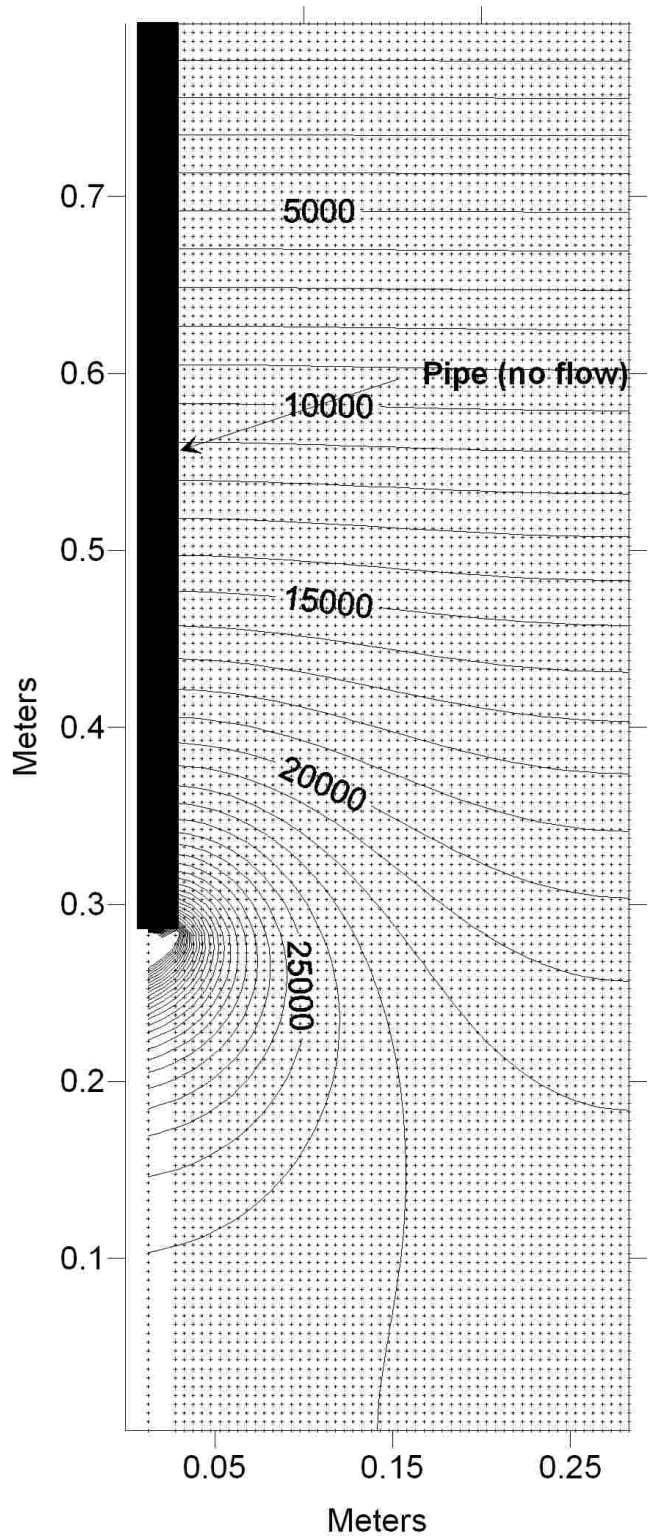

Figure 3-17. Illustration of the Finite Volume Grid Used for Drum Gas Flow Simulations. Pressure Contours Are in Pascals of Gage Pressure at Injection Pressure of 10 psig. Note: 1 psig = 6,895 Pa.

Drum Simulation Results and Pressure–Permeability Correlation

Simulations were run for effective gas conductivities ranging from 10^{-10} to 10^{-7} m/s (3.3×10^{-10} to 3.3×10^{-7} ft/s). The resulting correlation between effective gas permeability and gas flow rate is shown in Figure 3-18 and is described by

$$k_{eg} = 1.68 \times 10^{-12} \left(\frac{Q_{sc}}{\Delta P^2} \right) + 1.41 \times 10^{-16} \tag{3-6}$$

where Q_{sc} is in units of standard cm^3/min and pressure is in units of psi. In the case of INL Heel Grout specimen T6, simulations were run in which the cells at the drum wall were assigned a very high permeability to represent an annular space at the drum wall. The relationship between effective gas permeability and gas flow rate for specimen T6 is

$$k_{eg} = 1.2 \times 10^{-12} \left(\frac{Q_{sc}}{\Delta P^2} \right) \tag{3-7}$$

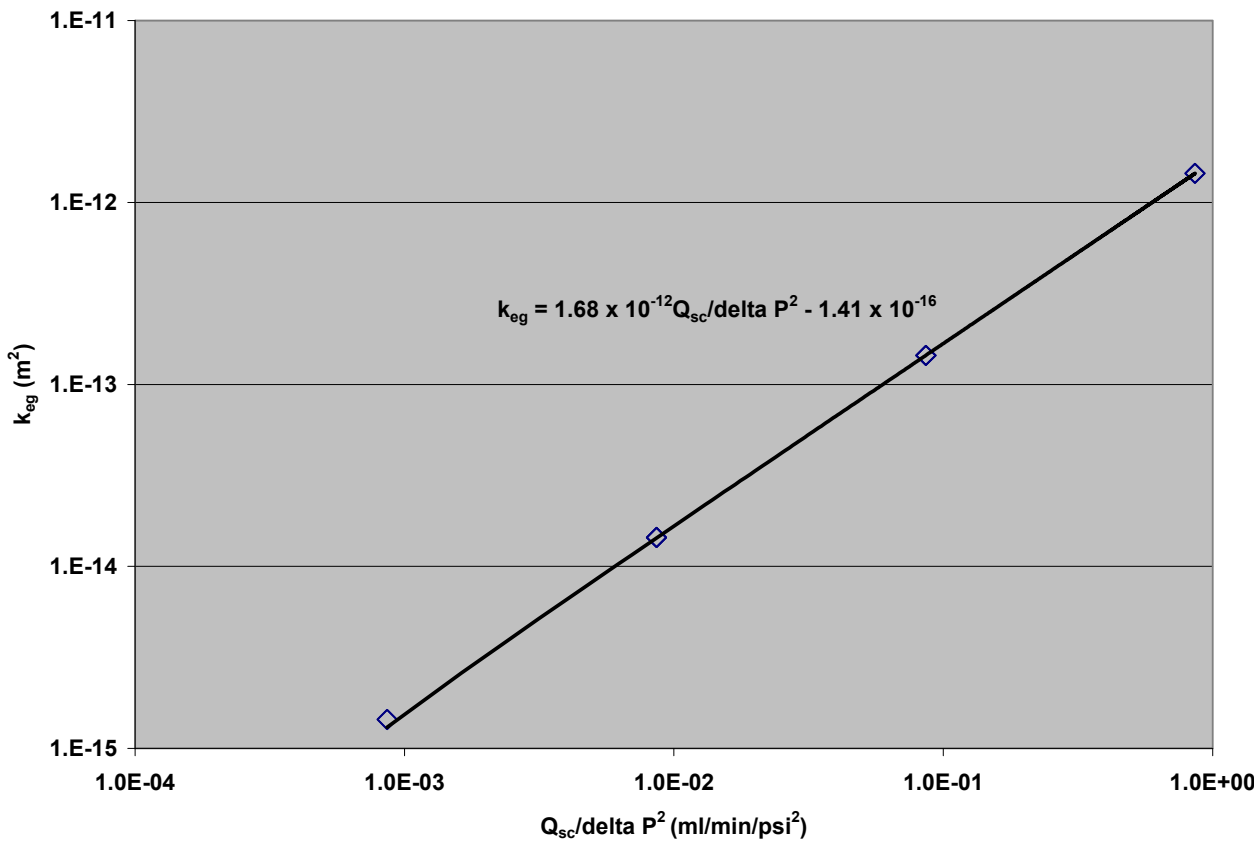

Figure 3-18. Correlation Between Gas Flow and Grout Effective Gas Permeability Developed for Drum Grout Specimens

Effective gas permeabilities were only estimated for the drum grout specimens that displayed some evidence of diffuse flow through the grout mass. The resulting permeability values are listed in Table 3-8 along with corresponding values of saturated hydraulic conductivity. Excluding the results for specimen T6, the estimated values of effective gas permeability are in the range of 10^{-16} to 10^{-14} m^2 [10^{-4} to 10^{-2} darcies] with corresponding saturated hydraulic conductivities in the range of 10^{-9} to 10^{-7} cm/s [10^{-11} to 10^{-9} ft/s]. The equivalent hydraulic conductivities are in the same range as those reported for SRS Alternative Reducing Grouts by Langton, et al. (2007). The specimens containing INL CLSM Grout (T7 and T8) have the lowest estimated gas permeabilities, whereas the specimens containing SRS Strong Grout have the highest (excluding consideration of drum grout specimen T6). Drum grout specimen T7, which was a monofill of INL CLSM, was the only specimen for which the gas injection tests did not show any evidence of annular flow around the injection pipe.

Table 3-8. Calculated Effective Gas Permeabilities for Selected Drum Grout Specimens

Drum	P_{inj} (psig)	P_A (psia)	Q (cm^3/min)	$\Delta(P^2)$ (psi^2)	k_{eg} (m^2)	K_{eg} (cm/s H_2O)
T1	14.0	14.43	5.4	600.1	1.5×10^{-14}	1.1×10^{-7}
	30.0	14.43	9.9	1766	9.6×10^{-15}	6.7×10^{-8}
	40.0	14.43	12.4	2755	7.7×10^{-15}	5.3×10^{-8}
	46.0	14.43	14.5	3444	7.2×10^{-15}	5.0×10^{-8}
	50.0	14.44	16.6	3944	7.2×10^{-15}	5.0×10^{-8}
				Mean:	*9.3×10^{-15}*	*6.6×10^{-8}*
				Standard Deviation:	*3.3×10^{-15}*	*2.6×10^{-8}*
T2	34.0	14.38	2.5	2134	2.1×10^{-15}	1.5×10^{-8}
	38.0	14.38	3.4	2537	2.4×10^{-15}	1.6×10^{-8}
	42.0	14.38	3.8	2972	2.3×10^{-15}	1.6×10^{-8}
	46.0	14.38	4.2	3439	2.2×10^{-15}	1.5×10^{-8}
	50.0	14.38	4.6	3938	2.1×10^{-15}	1.4×10^{-8}
				Mean:	*2.2×10^{-15}*	*1.5×10^{-8}*
				Standard Deviation:	*1.3×10^{-16}*	*8.4×10^{-10}*
T6	4.0	14.29	1301.7	130.3	1.2×10^{-11}	8.3×10^{-5}
	2.9	14.29	752.9	91.3	9.9×10^{-12}	6.9×10^{-5}
	4.35	14.29	1502.1	143.2	1.3×10^{-11}	8.7×10^{-5}
				Mean:	*1.6×10^{-11}*	*1.1×10^{-4}*
				Standard Deviation:	*2.1×10^{-12}*	*1.4×10^{-5}*
T7	40.0	14.29	0.0	2743	1.7×10^{-16}	1.2×10^{-9}
	44.0	14.29	0.1	3193	2.1×10^{-16}	1.4×10^{-9}
	46.0	14.28	0.3	3430	2.7×10^{-16}	1.9×10^{-9}
	48.0	14.28	0.4	3675	3.2×10^{-16}	2.2×10^{-9}
	50.0	14.28	0.4	3929	3.2×10^{-16}	2.3×10^{-9}
				Mean:	*2.6×10^{-16}*	*1.8×10^{-9}*
				Standard Deviation:	*6.7×10^{-17}*	*4.9×10^{-10}*
T8	44.0	14.30	0.03	3195	1.6×10^{-16}	1.1×10^{-9}
	48.0	14.30	0.09	3677	1.8×10^{-16}	1.3×10^{-9}
	50.0	14.30	0.02	3930	1.5×10^{-16}	1.0×10^{-9}
				Mean:	*1.6×10^{-16}*	*1.1×10^{-9}*
				Standard Deviation:	*1.5×10^{-17}*	*1.5×10^{-10}*

1 cm/s = 0.03281 ft/s
1 darcy = 0.9869×10^{-12} m^2

Drum grout specimen T6, which contained the monofill of INL Heel Grout, has the highest effective gas permeability. This specimen exhibited multiple gas flow pathways, including flow along the drum wall, and the simplified representation of the specimen in the numerical model does not fully capture the complex properties of this specimen.

4 CONCLUSIONS AND RECOMMENDATIONS

These mesoscale grout experiments provided staff with significant, first-hand knowledge of the various formulations DOE is considering for filling NDAA tanks and stabilizing tank wastes. This knowledge included information about mixing characteristics of grout formulations, the sensitivity of grout flow and water–solid segregation characteristics to the water-to-cement ratio, and lift interface characteristics and textures that develop as grout cures. These characteristics can all potentially affect the development and distribution of preferential flow pathways for the movement of water and gas in grout structures.

The experience gained when mixing grout for the mesoscale specimens indicates that the desired flowability of grout was generally achieved at a lower water-to-cement ratio than the nominal amount of water in DOE grout formulations indicated. In addition, the water required to achieve a specific flowability varied between batches and a slight excess of water led to segregation of water and grout solids. Although the lower water-to-cement ratios required for the grouts prepared for this study could be attributed to differences in the properties of the Portland cement, fly ash, and blastfurnace slag cement relative to the materials used by DOE, the variations in water-to-cement ratios between batches suggests careful quality control may be required during full-scale grout emplacement to maintain consistent grout properties. Excess water leading to segregation and bleeding from the mixture can produce layers of increased porosity and permeability within the grout mass. Such layering can provide permeable pathways for water and air to enter the grout mass and pathways for radionuclides to leave the grout. With regard to INL Heel Grout, batches mixed for this study did not exhibit the desired flow characteristic of self-consolidating cementitious material suitable for NDAA tank waste stabilization.

Visual observation of flow structures and surface textures that developed in the mesoscale specimens during grout emplacement and curing provided insight into the potential for such structures to develop in full-scale grout prototypes. Specific observations include flow structures around obstacles, such as pipes and other fixtures, vesicles and vugs within the grout mass, and significant void space that can develop when the topography of lower lifts is not filled in by grout during later lift emplacements. Such features may all contribute to development of preferential flow pathways as grout ages.

With respect to heat of hydration, conductive heat transfer, and temperature gradients, temperatures developed in the mesoscale specimens were relatively low (no more than approximately 56 °C [133 °F] and temperature differences between grout lifts were generally small. Although vertical temperature gradient absolute values as high as 78 °C/m [42.8 °F/ft] developed between thermocouples inside separate lifts, little evidence of thermal cracking was visible in the grout surfaces. Temperature data and direct observations also indicate that grout formulations having less Portland cement and more fly ash, blast furnace slag cement, or inert pea gravel (SRS Reducing, SRS Alternative 2, and INL CLSM and Heel Grouts) cured relatively slowly and remained gelatinous for more than 24 hours. This observation suggests that SRS Reducing Grout in a full-scale tank could be displaced if SRS Strong Grout emplacement follows on too quickly after the emplacement of SRS Reducing Grout.

Perhaps the most significant finding of this study was that annular gaps developed around pipes in nearly all the mesoscale specimens. Based on gas injection testing, annular gaps had apertures ranging from 3 to 9 μm [120 to 350 μin] in the drum grout specimens. The apertures of pipe annuli in the sector grout specimen ranged from approximately 14 to 20 μm [550 to 790 μin]. The larger annular apertures in the sector grout specimen (approximately three times those in the drum grout specimens) are attributed to its greater volume and more potential for drying shrinkage, consistent with the 3:1 ratio of the dimension of the sector grout specimen to the drum grout specimens.

Although the bulk effective gas permeabilities of the grout specimens estimated from the gas injection tests were in the range of 10^{-16} to 10^{-14} m^2 [10^{-4} to 10^{-2} darcies] with corresponding saturated hydraulic conductivities in the range of 10^{-9} to 10^{-7} cm/s [10^{-11} to 10^{-9} ft/s], similar to values reported for SRS alternative reducing grouts by Langton, et al. (2007), most of the tests were influenced by annular flow around the gas injection pipe. Thus, the bulk effective gas permeabilities may be overestimated. Visual inspection of the drum grout specimens did, however, reveal the presence of vesicles, vugs, and voids at lift separations that could be permeable pathways not penetrated by the gas injection pipes and thus not revealed by the gas injection tests.

Based on experience gained from these mesoscale grout monolith experiments and the limitations of these experiments, the following future actions are recommended to further investigate properties of DOE grout formulations and the effect of scale on the development of permeable pathways through large grout masses:

- Resolve uncertainties in the INL Heel Grout formulation, and perform additional tests to understand the unacceptable flow properties of the INL Heel Grout prepared for this study. This could include contacting DOE for clarification of the formulation.

- Repeat the gas injection tests after the grout specimens have aged for 6 to 9 months to investigate effects of long-term curing on grout properties.

- Perform additional gas permeability testing of the drum grout and sector grout specimens to better investigate the distribution of macrocracks and permeability within the specimens. This could be accomplished by small-drillhole minipermeametry or through coring the specimens for Hassler sleeve permeability tests of discrete grout intervals.

- Remove the metal drum from selected drum grout specimens, and inspect the specimens for lift separations. (Because the pneumatic testing method cannot detect the presence of internal annuli in the absence of external, permeable air pathways, additional methods for detecting internal annuli, such as physically exhuming the pipes and sectioning them for microscopic inspection, may later be required.)

- Construction of a larger scale, cylindrical specimen with grout lifts emplaced using a grout pump in a manner similar to that which may be used to place grout in the NDAA tanks would provide a better representation of the permeability structure in the full-scale tanks. Experience gained when constructing the sector grout specimen, and the presence of voids and lift contact separations revealed by visual inspection of the sector specimen suggest that the internal structure of large-scale grout masses will depend on the manner in which grout is emplaced. Construction of the larger-scale specimen will

better inform evaluations of the potential for permeable pathways to be present in the full-scale NDAA tanks.

- Prepare specimens with more closely spaced thermocouples, and apply an external heat source to rapidly initiate thermal hydration of slag cement and fly-ash containing batches and maintain them at higher temperatures during curing to better estimate the effect of large thermal gradients on cracking due to thermal stresses. Despite the apparent absence of thermally induced cracks on the surfaces of the drum and sector grout specimens, the strongest thermal gradients were between grout lifts that were subsequently covered by the last lift and thus not available for visual inspection. In addition, only approximate estimates of thermal gradients could be made because of the relatively coarse spacing of thermocouples. The test results can be compared to the results of thermo-mechanical modeling and can validate models of full-scale grout emplacements. These tests will better inform evaluations of the potential for thermal cracking in the full-scale NDAA tanks.

- Measure diffusion rates in laboratory-scale grout samples. The tests could involve both conservative and nonconservative tracers, including radionuclides. Experiments would involve intact grout samples; samples known to contain fractures, voids, or annuli; and samples with artificial fractures. Data from these tests would supplement existing data on diffusion coefficients measured primarily on bench-scale specimens.

- Perform tracer tests on laboratory-scale and mesoscale grout samples. The tests would focus on tracer (e.g., dye) transport through fractures, fractured grout, and void-containing grout; along annuli; and by interaction with adjacent grout matrix. These tests will elucidate the three-dimensional permeability structure of the grout and inform transport model design.

- Characterize the solid-phase assemblages in grout samples representing varying conditions and locations. These data will inform evaluation of chemical reactions potentially affecting radionuclide mobility in the grout.

5 REFERENCES

Bird, R.B., W.E. Stewart, and E.N. Lightfoot. *Transport Phenomena.* New York City, New York: John Wiley & Sons. 1960.

Brooks, R.H. and A.T. Corey. "Properties of Porous Media Affecting Fluid Flow." *Journal of Irrigation and Drainage Division, American Society of Civil Engineers*. Vol. 92 (IR2). pp. 61–88. 1966.

CH2M WG Idaho, LLC. "Construction Specification Project No. 15722 INTEC Grout and CLSM Supply Project." SPC–763. Idaho Falls, Idaho: CH2M WG Idaho, LLC. March 23, 2007.

Kilburn, C.R.J. *Active Lavas*. London, England: Taylor & Francis. p. 374. 1993.

Kutzner, C. *Grouting of Rock and Soil.* London, England: Taylor & Francis. p. 271. 1996.

Langton, C.A. and J.R. Cook. "Recent Progress in DOE Waste Tank Closure." Waste Management Symposium 2008, February 24–28, 2008, Phoenix, Arizona. WSRC–STI–2007–00686. Aiken, South Carolina: Washington Savannah River Company. 2008.

Langton, C.A., A. Ganguly, C.A. Bookhammer, M. Koval, and W.L. Mhyre. "Grout Formulations and Properties for Tank Farm Closure (U)." WSRC–STI–2007–00641. Rev. 0. Aiken, South Carolina: Washington Savannah River Company. 2007.

Neville, A.M. *Properties of Concrete.* London, England: Prentice Hall. 2006.

Skolnik Industries. "Open and Tight Head Carbon Steel Drums." <http://www.skolnik.com/carbon.shtml> Chicago, Illinois: Skolnik Industries. 2008. (03 June 2009).

Walter, G.R. "BioGas Emissions Model (BIGEM) Version 1.00 Software Validation Test Plan and Report." San Antonio, Texas: CNWRA. 2005.

Walter, G.R. and C.L. Dinwiddie. "Conceptual Design for Small-Scale Grout Monolith Tests." San Antonio, Texas: CNWRA. April 2008.

APPENDIX A

Table A–1. Grout Drum Batch Details

Savannah River Site (SRS) Reducing Grout Materials for 3-ft^3 Batches	Nominal Quantity	T2-1	T3-1	T3-2	T3-3
Portland Type I/II Cement (lbm)	8.4	8.9	8.4	8.9	8.9
Silica Sand ASTM C–33 (lbm)	254.3	254.4	256.0	254.4	254.4
Ground Granulated Blast-Furnace Slag Cement Grade 120 ASTM C989 (lbm)	22.4	22.4	22.4	22.6	22.4
Fly Ash Class F (lbm)	41.1	41.2	41.1	41.2	41.2
Water (gal)	6.70	5.18	4.90	4.95	5.10
ADVA 380 High-Range Water Reducer (ml)	272.0	270	270	270	270
Viscofier Kelco-crete® (gm)	30.6	30.2	29.5	30.0	30.0
Sodium Thiosulfate, Pentahydrate (gm)	102.1	90.68	92.10	90.70	90.70
H_2O:[cement + fly ash] (−)	0.78	0.60	0.57	0.57	0.59
ASTM-6103-04 Flow Test Diameter (in)	≥11.0	11.0	11.5	11.0	11.0
Bulk Density (kg/m^3)	—	2121	2169	2115	2147

SRS Strong Grout Materials for 3-ft^3 Batches	Nominal Quantity	T1-1	T1-2	T1-3	T2-2	T2-3	T9-1	T9-2	T9-3
Portland Type I/II Cement (lbm)	61.1	61.5	61.4	61.4	61.2	61.4	61.1	61.5	60.4
Silica Sand ASTM C–33 (lbm)	253.9	253.9	253.8	254.0	254.0	254.0	253.9	254.0	254.0
Water (gal)	5.20	5.34	4.92	5.09	4.92	5.58	5.11	5.33	5.20
ADVA 380 High-Range Water Reducer (ml)	302.6	302.0	302.0	303.0	302.0	302.0	302.0	302.0	302.0
Viscofier Kelco-crete® (gm)	12.0	12.1	12.2	12.1	12.2	12.3	12.0	12.2	12.2
H_2O:cement (−)	0.71	0.73	0.67	0.69	0.67	0.76	0.70	0.73	0.73
ASTM–6103–04 Flow Test Diameter (in)	≥11.0	11.0	11.0	11.0	11.0	11.0	11.0	11.0	11.0
Bulk Density (kg/m^3)	—	2188	2208	2149	2202	2185	2210	2199	2199

SRS Alternative 1 Grout Materials for 3-ft^3 Batches	Nominal Quantity	T4-1	T4-2	T4-3	T11-1	T11-2	T11-3
Portland Type I/II Cement (lbm)	33.7	33.8	33.6	34.1	34.1	33.8	33.6
Silica Sand ASTM C–33 (lbm)	157.1	157.2	157.2	157.2	157.2	157.2	157
Ground Granulated Blast-Furnace Slag Cement Grade 120 ASTM C989 (lbm)	33.7	33.6	33.8	33.8	33.8	35.4	33.6
Fly Ash Class F (lbm)	87.9	87.8	88.0	88.0	88.0	86.4	87.8
Water (gal)	7.0	6.5	6.59	5.97	6.1	6.38	6.02
ADVA 380 High-Range Water Reducer (ml)	161.5	162.0	162.0	162.0	162.0	162.0	162.0
Viscofier Kelco-crete® (gm)	23.80	23.80	23.81	23.81	23.80	23.80	23.80
Sodium Thiosulfate, Pentahydrate (gm)	102.1	90.71	90.69	90.73	90.68	90.74	90.71
Hydration Stabilizer RECOVER (ml)	32.6	33.0	33.0	33.0	33.0	33.0	33.0
H_2O:[cement + fly ash] (−)	0.38	0.35	0.35	0.32	0.33	0.34	0.32
ASTM 6103-04 Flow Test Diameter (in)	≥11.0	11.0	10.8	11.0	11.0	11.0	11.0
Bulk Density (kg/m^3)	—	2048	2057	2055	2074	2080	2051

Table A–1. Grout Drum Batch Details (continued)

SRS Alternative 2 Grout Materials for 3-ft^3 Batches	Nominal Quantity	T5-1	T5-2	T5-3	T12-1	T12-2	T12-3
Portland Type I/II Cement (lbm)	20.6	21.1	21.1	21.1	21.1	21.1	21.1
Silica Sand ASTM C–33 (lbm)	104.7	104.8	104.8	104.8	104.6	104.8	104.8
Ground Granulated Blast-Furnace Slag Cement Grade 120 ASTM C989 (lbm)	28.0	28.0	28.0	28.0	28.0	28.0	28.0
Fly Ash Class F (lbm)	93.5	93.6	93.6	93.6	93.6	93.4	93.6
No. 8 Aggregate 3/8 in stone (lbm)	176.9	177.0	177.0	177.0	177.0	176.8	177.0
Water (gal)	6.70	5.76	5.62	6.25	5.70	6.15	5.88
ADVA 380 High-Range Water Reducer (ml)	161.5	162.0	162.0	162.0	162.0	162.0	162.0
Viscofier Kelco-crete® (gm)	23.8	23.79	23.8	23.8	23.8	23.8	23.81
Sodium Thiosulfate, Pentahydrate (gm)	102.1	90.73	90.72	90.72	90.74	90.74	90.74
Hydration Stabilizer RECOVER (ml)	32.6	33.0	33.0	33.0	33.0	33.0	33.0
H_2O:[cement + fly ash] (−)	0.39	0.34	0.33	0.37	0.33	0.36	0.34
ASTM 6103-04 Flow Test Diameter (in)	≥11.0	11.0	10.8	10.5	11.0	10.3	11.0
Bulk Density (kg/m^3)	—	2197	2044	2141	2201	2116	2161

Idaho National Laboratory (INL) Heel Grout Materials for 3-ft^3 Batches	Nominal Quantity	T6-1	T6-2	T6-3	T8-1
Portland Type I/II Cement (lbm)	25.2	25.2	25.2	25.2	25.2
Silica Sand ASTM C–33 (lbm)	276.3	276.4	276.4	276.4	276.4
Ground Granulated Blast-Furnace Slag Cement Grade 120 ASTM C989 (lbm)	38.9	39.0	39.0	39.0	39.0
Fly Ash Class F (lbm)	13.1	13.2	13.2	13.2	13.2
Water (gal)	4.10–5.9	4.38	4.63	4.58	4.50
ADVA 380 High-Range Water Reducer (ml)	80.5–262.9	103.5	81.0	105.0	111.0
H_2O:[cement + fly ash] (−)	0.44	0.47	0.50	0.49	0.48
ASTM C–143 Slump Flow Test Diameter (in)	6.0–11.0	8.5	6.5	9.0	8.5
Bulk Density (kg/m^3)	—	2059	2197	2016	2078

INL Controlled Low Strength Material (CLSM) Grout Materials for 3-ft^3 Batches	Nominal Quantity	T7-1	T10-1	T7-1 & T10-1 Split
Portland Type I/II Cement (lbm)	33.3	33.2	33.2	33.4
Silica Sand ASTM C–33 (lbm)	209.6	209.6	209.6	209.8
Fly Ash Class F (lbm)	22.2	22.2	22.2	22.2
Water (gal)	4.20	3.98	3.70	3.70
ADVA 380 High-Range Water Reducer (ml)	312.3	312.0	312.0	312.0
H_2O:[cement + fly ash] (−)	0.63	0.60	0.56	0.55
ASTM–6103–04 Flow Test Diameter (in)	≥11.0	11.0	10.5	10.2
Bulk Density (kg/m^3)	—	2259	2254	—

INL CLSM Grout Materials for 3.45-ft^3 Batch	Nominal Quantity	T8-2
Portland Type I/II Cement (lbm)	38.3	38.4
Silica Sand ASTM C–33 (lbm)	241.0	241.0
Fly Ash Class F (lbm)	25.6	25.6
Water (gal)	4.9	4.3
ADVA 380 High-Range Water Reducer (ml)	359.2	359.0
H_2O:[cement + fly ash] (−)	0.63	0.56
ASTM 6103-04 Flow Test Diameter (in)	≥11.0	10.5
Bulk Density (kg/m^3)	—	2262

INL CLSM Grout Materials for 3.9-ft^3 Batches	Nominal Quantity	T7-2	T7-3	T8-3	T10-2	T10-3
Portland Type I/II Cement (lbm)	43.3	43.4	43.2	43.2	43.4	43.2
Silica Sand ASTM C–33 (lbm)	272.5	272.4	272.6	272.6	272.4	272.6
Fly Ash Class F (lbm)	28.9	28.8	29.0	29.0	28.8	29.0
Water (gal)	5.5	4.45	4.56	4.53	4.36	4.4
ADVA 380 High-Range Water Reducer (ml)	406.0	404.0	406.0	406.0	600.0	406.0
H_2O:[cement + fly ash] (−)	0.63	0.51	0.53	0.52	0.50	0.51
ASTM-6103-04 Flow Test Diameter (in)	≥11.0	10.0	10.5	10.0	10.0	10.5
Bulk Density (kg/m^3)	—	2264	2268	2230	2268	2289

Table A–2. Grout Sector Batch Details

Savannah River Site (SRS) Reducing Grout Materials for 6-ft^3 Batches	Nominal Quantity	Lift 1, A	Lift 1, B	Lift 1, C
Portland Type I/II Cement (lbm)	16.8	18.0	18.0	18.0
Silica Sand ASTM C–33 (lbm)	508.6	508.6	508.6	508.6
Ground Granulated Blast-Furnace Slag Cement Grade 120 ASTM C989 (lbm)	44.9	45.0	45.0	45.0
Fly Ash Class F (lbm)	82.3	82.4	82.2	82.3
Water (gal)	13.5	9.75	8.81	9.38
ADVA 380 High-Range Water Reducer (ml)	544.0	544.0	544.0	544.0
Viscofier Kelco-crete® (gm)	61.2	61.2	61.2	61.2
Sodium Thiosulfate, Pentahydrate (gm)	204.1	0.40	0.40	0.40
H_2O:[cement + fly ash] (−)	0.78	0.56	0.51	0.54
ASTM 6103-04 Flow Test Diameter (in)	≥11.0	10	10.5	11
Bulk Density (kg/m^3)	—	2122.2	1993.6	1957.4

SRS Reducing Grout Materials for Short Batch	Nominal Quantity	Lift 1, D
Portland Type I/II Cement (lbm)	10.1	10.0
Silica Sand ASTM C–33 (lbm)	305.3	305.9
Ground Granulated Blast-Furnace Slag Cement Grade 120 ASTM C989 (lbm)	26.9	27.0
Fly Ash Class F (lbm)	49.4	49.4
Water (gal)	8.1	5.63
ADVA 380 High-Range Water Reducer (ml)	326.4	326.0
Viscofier Kelco-crete® (gm)	36.7	36.7
Sodium Thiosulfate, Pentahydrate (gm)	122.5	122.5
H_2O:[cement + fly ash] (−)	0.78	0.54
ASTM 6103-04 Flow Test Diameter (in)	≥11.0	11.0
Bulk Density (kg/m^3)	—	1998.9

SRS Strong Grout Materials for 6-ft^3 Batches	Nominal Quantity	Lift 1	Lift 2 A	Lift 2 B	Lift 2 C	Lift 2 D	Lift 3 A	Lift 3 B	Lift 3 C	Lift 3 D
Portland Type I/II Cement (lbm)	122.2	122.7	122.7	122.7	122.7	122.7	122.7	122.7	122.7	122.7
Silica Sand ASTM C–33 (lbm)	507.8	507.8	507.8	507.8	507.8	508.4	507.8	507.8	507.8	507.8
Water (gal)	10.4	10.08	10.78	9.75	10.50	11.25	10.50	10.12	10.63	10.44
ADVA 380 High-Range Water Reducer (ml)	605.2	605.0	605.0	605.0	605.0	605.0	605.0	605.0	605.0	605.0
Viscofier Kelco-crete® (gm)	24.0	24.0	24.0	24.0	24.0	24.0	24.0	24.0	24.0	24.0
H_2O:[cement] (−)	0.71	0.68	0.73	0.66	0.71	0.76	0.71	0.69	0.72	0.71
ASTM–6103–04 Flow Test Diameter (in)	≥11.0	11.0	11.0	11.0	11.0	11.0	11.0	11.0	11.0	11.0
Bulk Density (kg/m^3)	—	2076	1981	2070	2025	2047	1989	2034	2179	2090

Table A–3. Idaho National Laboratory (INL) Pipe Grout Batch Details

INL Pipe Grout Materials for 0.08-ft^3 Batch	Nominal Quantity	INL-P
Portland Type I/II Cement (lbm)	20.5	20.6
Fly Ash Class F (lbm)	48.8	48.8
Water (gal)	3.0	2.31
ADVA 380 High-Range Water Reducer (ml)	53.7	54.0
H_2O:[cement + fly ash] (−)	0.36	0.28
ASTM-6103-04 Flow Test Diameter (in)	≥11.0	12.0 to 13.5
Bulk Density (kg/m^3)	—	1810